ELSEVIER

Journal of Alloys and Compounds 229 (1995) 175–205

Journal of ALLOYS AND COMPOUNDS

The electrochemical synthesis of telluride Zintl anions

Christopher J. Warren[a], Robert C. Haushalter[b,*], Andrew B. Bocarsly[c]

[a]*Department of Chemistry, Cornell University, Ithaca, NY 14853, USA*
[b]*NEC Research Institute, 4 Independence Way, Princeton, NJ 08540, USA*
[c]*Department of Chemistry, Princeton University, Princeton, NJ 08544, USA*

Received 31 March 1995

Abstract

A novel electrochemical synthetic technique has been developed recently for the generation of heteropolyatomic Zintl anion clusters via the cathodic dissolution of telluride electrodes. Whereas previous synthetic techniques for the generation of these compounds have relied on high temperature fusion of the elements and/or extraction methods, this technique simply relies on the constantly increasing concentration of anions as they are discharged from a cathode, is performed at room temperature and in many cases yields X-ray quality single crystals in as little as 3–5 days. In the process of our study of this technique, it has also been shown that it allows for the preparation of Zintl anions which have not been and may not be accessible by these standard high temperature and extraction techniques. The versatility of this synthetic technique has been demonstrated by the isolation of small six- to seven-atom anions, larger 15-atom cluster anions and one-dimensional chain materials from the Au, Ga, In, Sn, As and Sb telluride systems. Ongoing research suggests that the synthesis of additional materials should be possible.

Keywords: Electrochemical synthesis; Telluride; Zintl anions

1. Introduction

The primary route to the preparation of intermetallic alkali and alkaline earth compounds with metals, semimetals and heavy main group non-metals has been through the use of the high temperature fusion of stoichiometric mixtures of these elements [1]. This technique, first developed in the late 1960s and used extensively in Germany by Schäfer, von Schnering, Nesper and Eisenmann, involves the direct combination of the elements in a classic solid state high temperature fusion reaction. The reactions take place under inert atmospheres in sealed metal or quartz ampoules at relatively high temperatures. In fact, these reactions typically take place with such explosive violence caused by local overheating that temperatures of between 1200 and 1300 K can easily be produced in the reaction zone [1c]. Oxide layers may also build up on the metals prior to the syntheses, thus requiring the use of unsuitably high temperatures for starting off the reaction in the first place. This technique also requires carefully conducted cooling and annealing experiments aimed at producing single-crystal products which can be isolated from the melt. When attempting these types of synthesis, one must also consider the possible products that can be formed, for even the phase diagrams of the simple binary systems typically consist of multiple phases. This presents problems for the production of single-phase products and interferes with the characterization process which relies heavily on powder X-ray diffraction studies. When an unknown system is examined for the first time, particularly one where ternary products are sought, the method usually yields mixtures of compounds. If one is lucky enough to obtain single-crystal products, which can be obtained through tedious variations in the stoichiometries of the reactants, then structural characterization of these products can lead to a better understanding of the system and experiments aimed at obtaining a homogeneous product. In most cases where this technique is used, however, it is only these crystalline products that are identified, and the majority of these reactions are, subsequently, incompletely characterized.

* Corresponding author.

SSDI 0925-8388(95)01710-0

Another technique for the isolation of stable crystalline derivatives of Zintl anions, which was first used in the early 1970s by Kummer and Diehl for the successful isolation of a stable derivative of Sn_9^{4-}, has been used more recently in the USA by Corbett, Ibers and Haushalter and involves the solvent extraction of alloy phases [2]. Zintl, and others even before him, had demonstrated that alloys of the alkali and alkaline earth metals with the heavier main group and post-transition metals were soluble in basic polar media. Their dissolution into these media led to intensely colored solutions which were only incompletely characterized by potentiometric and conductometric titration studies, as crystalline products were never isolated. Since these Zintl anions can be considered extremely good reducing agents (typically 3- to 5-), the reversion of the salt phase (present in solution) to a metallic-looking phase (present on evaporation of the solvent) can be viewed as the result of a delocalization of electrons from the anions back onto the cations. Hence, the key to isolating single-crystal samples lay in finding a way to prevent (or at least to slow down) this process, and this way was found by Corbett through the use of the macrobicyclic aminopolyether 4, 7, 13, 16, 21, 24-hexaoxa-1, 10-diazobicyclo-[8.8.8]hexacosane (referred to hereafter as 2,2,2-crypt) [3]. This octadentate ligand demonstrates an extremely strong complexing ability to the alkali cations of sodium, potassium and rubidium (the formation constants vary from 10^4 to 10^{10}) and has been found to enhance greatly the solubility of these metals in liquid ammonia, amines and ethers [4].

The first use of 2,2,2-crypt as a stabilizing agent for Zintl anions was attempted by Corbett et al. [2x] in which the polyantimonide anion Sb_7^{3-} was isolated as the crystalline cryptated salt $[Na\text{-}(2,2,2\text{-crypt})]_3Sb_7$. The reaction was done by dissolving a powdered alloy of nominal composition NaSb in an ethylenediamine solution containing one third of an equivalent of crypt. The resulting dark-red–brown solution was then decanted from the unreacted alloy (not all was soluble) and slowly evaporated under vacuum over a period of about 12 h. Dark-red–brown needle-shaped (and reasonably stable) crystals were obtained from the reaction and characterized by single-crystal X-ray diffraction. Alloys of compositions ranging from Na_3Sb to $NaSb_3$ gave only the single-phase product $[Na(2,2,2\text{-crypt})]_3Sb_7$, which was hailed as the first stable compound containing a homopolyatomic anion of a metal to be characterized by means of a complete crystal structure.

Using complexed cations as counterions, it soon became possible to crystallize the anions Ge_4^{2-}, Ge_9^{2-}, Ge_9^{4-}, Sn_4^{2-}, Sn_5^{2-}, Sn_9^{3-} Sn_9^{4-} and Pb_5^{2-} from similar extractions of group 14 alloy phases [2]. Through an intensive study of alkali metal alloys of arsenic, antimony, bismuth, selenium and tellurium (as well as many mixed-metal systems) in anhydrous liquid ammonia and ethylenediamine, Corbett et al. were able to isolate brightly colored crystalline salts on solvent removal, rather than the amorphous intermetallic materials that Zintl obtained.

Since the initial work of Corbett et al., other tetraalkylammonium cations have been used successfully in the isolation of stable solid derivatives of Zintl anions [2]. Sufficient structures had been done to realize that the larger cations such as crypt, while they worked well for the isolation of crystalline products, tended to dominate the crystal packing, leading to a greater tendency of the anions in the structure to be disordered. The use of smaller cations (such as the family of tetraalkylammoniums) was believed not only to reduce the possibility of anion disorder but also to aid in the formation of more extended or even three-dimensional materials rather than the highly charged isolated anionic moieties which are invariably isolated using 2,2,2-crypt. To date, however, no one working in this field has been able to produce these extended structures through the solvent extraction of alloy phases.

Both the high temperature fusion reactions and the extraction technique have been extremely successful as routes to the isolation of stable, solid derivatives of the homopolyatomic and heteropolyatomic anions of the heavier main group and post-transition metals. They have led to the isolation of literally hundreds of these Zintl compounds and have given us a greater understanding of the structures and bonding schemes present in them.

Several other solid state techniques including reactions in molten salts [5], arc melting [6], chemical transport reactions [7], molecular beam methods [8] and reactions done under extremely high pressures [9] have all been used for the synthesis of intermetallic Zintl compounds. These rather specialized techniques are usually limited in their applications to a particular system and do not enjoy the extremely high success rate of that of the high temperature elemental fusion process. Nevertheless, as new synthetic reagents become available, our knowledge of the reaction steps and mechanisms involved becomes more complete, and crystallography and other forms of spectroscopy become easier to do, the development of these and other new methods should lead to the isolation of many more of these Zintl compounds and expand this intriguing area of solid state chemistry. One such method that has been developed in our laboratory is the electrochemical synthesis of Zintl anion clusters through the electrochemically controlled cathodic dissolution of alloy electrodes [10]. This technique has enjoyed a great deal of success, yielding not only molecular species, but also one-dimensional inorganic

polymers and even pseudo-two-dimensional materials. Variations on the experimental technique show that it is versatile, having been shown to produce single-crystal samples for the majority of main group binary tellurides.

2. Characterization of Zintl compounds

The characterization of Zintl compounds has primarily relied on crystallographic methods using a combination of both single-crystal X-ray analysis and X-ray powder diffraction. Indeed, the use of single-crystal X-ray diffraction is invaluable for the identification of solids for it usually gives conclusive evidence of the structure of a compound provided that single-crystal samples can be made. In the event that they cannot, a number of other techniques have been used for the indirect characterization of Zintl compounds and deserve mention.

Zintl himself used a combination of potentiometric titrations and conductance measurements to identify the anionic species present in his liquid ammonia solutions. More recently, a combination of electrochemical methods and nuclear magnetic resonance (NMR) studies have been used both to generate and to study these unusual species in liquid ammonia and ethylenediamine solutions. For example, Rudolph and coworkers [11] have electrochemically generated Zintl anions of the form $Sn_{9-x}Pb_x^{4-}$ ($x = 0$–9) from the cathodic dissolution of 1:1 Sn:Pb alloy electrodes. Although single-crystal samples were not obtained from the electrolyses, subsequent NMR studies (using ^{119}Sn and ^{207}Pb nuclei) suggested that all the possible anions in this series were present in the catholyte solution. NMR measurements were used not only to confirm their presence but also to demonstrate that the least entropic species (Sn_9^{4-} and Pb_9^{4-}) were predominant (as evidenced by the relative intensities of their signals compared with the heteropolyatomic moieties). Although this technique appeared promising in the tin–lead system, it was unfortunately not pursued with any other systems.

More recently, Schrobilgen and coworkers [12] have used multinuclear NMR spectroscopy as a complementary tool to X-ray crystallography in order to study an entire series of the homopolychalcogenide and heteropolychalcogenide anions of selenium and tellurium, as well as the mixed-metal Zintl anions $Sn_2X_3^{2-}$, $Pb_2X_3^{2-}$, $Tl_2X_2^{2-}$, HgX_2^{2-}, CdX_2^{2-}, TlX_3^{3-}, $Tl_2X_2^{2-}$ (X = Se and/or Te). The use of this technique is particularly well suited to the study of the solution chemistry of these Zintl anions since every post-transition metal element forming one of these Zintl phases possesses at least one natural abundance isotope that is NMR active. The NMR studies of Schrobilgen and coworkers, for example, were done using a combination of the spin $\frac{1}{2}$ nuclei ^{77}Se, $^{117,119}Sn$, ^{125}Te, ^{207}Pb, ^{199}Hg, ^{113}Cd and $^{203,205}Tl$. Many of the compounds that Schrobilgen and coworkers characterized in solution were also obtained in crystalline form, allowing for the direct correlation of NMR signals to confirmed structures. Since all the NMR nuclei that Schrobilgen and coworkers used were spin $\frac{1}{2}$, they were capable of providing additional valuable structural information for those compounds that were not characterized by single-crystal analysis, by virtue of their heteronuclear and homonuclear spin–spin couplings.

Although used in a limited sense for the identification of a particular isolated fragment that might be present in a given Zintl compound, IR spectroscopy studies are generally not very informative in the overall structural characterization of Zintl compounds. This especially true for those compounds containing organic cations where the mid-IR region is invariably dominated by absorption from the hydrocarbon skeletons of the tetraalkylammonium cations. Metal–metal bond absorptions are expected to fall in the far-IR region of 200–400 cm^{-1} but, owing to the paucity of studies done, caution must be taken in assigning these stretches to a particular mode in the absence of any systematic studies using isotope labeling.

The techniques of UV and visible spectroscopy are also generally of little use in identifying Zintl compounds. Here the problem is twofold. The first and most obvious problem is that, while the structures of the Zintl anions may have been exactly determined by X-ray crystallography studies, these studies have been conducted with the sample in crystalline form. There is no reason to believe that these compounds will have the same structures when dissolved in a given solvent and, in fact, it has been shown that many of these compounds do not retain their identity in solution [13a,b]. The second problem is that even if the compounds remain intact in the solvent, they typically show featureless UV–visible spectra that yield no information about the coordination environment of the metal ions [13c, d]. Some UV–visible experiments, particularly those of the transition metal tellurides, display a UV–visible range that is entirely silent.

3. Why tellurides?

Given the enormous range of potential electrode materials, an obvious question is why choose the metal tellurides? In answer to this question, one must consider that these metal telluride compounds have considerable industrial usage, especially in low band gap

semiconductors, photovoltaics and IR detection devices [14]. There is therefore a general impetus to find a synthetic route to their preparation. However, one of the main reasons that the chemistry of the metal tellurides has not been fully investigated until recently is the lack of such a suitable technique, which is also convenient and avoids the hazards and dangers associated with these toxic substances. Traditionally, the approaches to the syntheses of metal sulfides, selenides and tellurides have typically concentrated on the use of the dihydrogen gases, such as H_2S and H_2Se. These gases were bubbled into reaction vessels to undergo chemical reactions. The obvious problem with these reactions, however, is that both H_2S and H_2Se are extremely toxic, malodorous and expensive, and the reactions done using them often lead to impure mixtures of products [15]. Even more of a problem is hydrogen telluride (H_2Te), which not only suffers from all the above disadvantages but also is unstable at room temperature, decomposing into hydrogen gas and tellurium metal. While the solution chemistry of telluride compounds (using telluride Zintl phases in anhydrous solvents) has been explored as an alternative to the use of hydrogen telluride gas [16], a serious limitation to this technique is the generation of neutral organic species such as $(CH_3)_2Te$ or $(C_2H_5)_2Te$ which are also extremely toxic and malodorous. Because of the nature of the electrochemical experiments discussed herein, which are done in tetraalkylammonium salts such as $(CH_3)_4N^+$ and $(C_2H_5)_4N^+$, these species will invariably be generated; so appropriate cautions must be considered when attempting the cathodic dissolution reactions.

From a practical viewpoint, the use of congruently melting telluride phases (as opposed to selenide or sulfide phases) in the electrochemical synthesis of Zintl anions was chosen for three main reasons. The first is that, in order for a cathode to work, it must be able to conduct electricity. Since tellurium lies on the metalloid border, the binary heavier main group and post-transition metal alloys that contain it should be conductoring (or at least semiconductors). The second reason is that, when compared with the Zintl anions containing sulfur and selenium, there are far fewer telluride Zintl anions reported in the literature; so the success rate of the technique would be further increased by producing new anions, and not just reproducing known anions. The third reason to use tellurium in the electrochemical synthesis is that compounds made with this element have been shown to be less sensitive to impurities in the solvent. This is because tellurium is more electronegative than the other heavier main group elements (such as tin and lead) and is therefore not as strong a reducing agent. Tellurides can also disproportionate in solution (two Te_2^{2-} anions can each lose an electron and combine to form the Te_4^{2-} species) whereas the tin and lead clusters do not have that capability. For these reasons, telluride Zintl anions should not be as easily oxidized by the impurities that can be present in the ethylenediamine or supporting electrolytes, allowing single-crystal materials to grow without decomposition.

4. Description of the experimental technique

4.1. Background and significance

Apart from the early electrolyses of Zintl and the more recent rather limited electrosynthetic and NMR studies by Rudolph and coworkers, utilization of the electrochemically controlled cathodic dissolution of alloys to prepare structurally characterized solids appears uninvestigated. Zintl and coworkers [17] used only pure element electrodes in their electrolyses (Tl, Ge, Sn and Pb), which did not, in general, work well and in no case yield single-crystal products. The studies of Rudolph and coworkers [11] led to the electrochemical generation of Sn–Pb clusters which were characterized by NMR studies, but they too either were not able to or did not try to isolate crystalline derivatives.

The use of the highly reactive alkali metal alloys of the heavier main group elements and post-transition metals, whether they be made by the high temperature fusion technique and crystallized on cooling, or used in combination with organic cations as extracts in ethylenediamine, continues to be the most popular and widely used technique for the synthesis of Zintl anion clusters. However, rather than using these extremely reactive alkali metal alloy phases which are both difficult to synthesize and troublesome to work with, the objective in the electrochemical experiments presented herein was to replace them with the non-reactive, congruently melting binary telluride phases which do not contain alkali metals. These binary telluride alloys are easily prepared from the fusion of stoichiometric amounts of the pure elements or can be purchased directly as the compounds from a suitable chemical distributor. Unlike their corresponding alkali metal derivatives, these binary telluride phases are stable in the atmosphere and to not suffer from any of the back-electron transfer problems associated with the alkali metal derivatives. Once obtained, these alloys can then be used as cathodes in an electrochemical cell where a current will be applied to generate anions. Hence, one can imagine that, instead of using the highly reactive alkali metal alloy of, say, composition $K_3Sb_2Te_3$ to generate antimony telluride anions on its dissolution into ethylenediamine, an electrode of composition Sb_2Te_3 to which a cathodic current will be applied can generate these antimony

telluride anions electrochemically. Thus, instead of dissolving the highly reactive alkali metal alloys and producing Zintl anions by a chemical method, application of current to the non-reactive binary telluride alloy will generate Zintl anions by an electrochemical method. Once generated, these Zintl anions can then be crystallized with the cations that will conveniently be present in the supporting electrolyte.

The electrochemical synthetic technique presented herein has proven useful for the generation of a wide variety of Zintl anion clusters and has several advantages over the existing high temperature fusion and extraction techniques. For one, the electrochemical reactions will not suffer from the extreme dangers associated with making the alkali metal alloys. Also, these reactions will be run at room temperature, and can be done right on the benchtop. However, most importantly, this electrochemical technique will generate new Zintl anions (as will be shown in the following sections) which have not been, or may never be, synthesized by the high temperature fusion method or through the extraction of alloy phases.

4.2. The electrochemical cell

The electrochemical cells used were fashioned from glass screw-thread tubes and fine porosity Pyrex frits. They have essentially the same characteristic form of a standard H-type electrochemical cell, with some minor modifications. The cell consists of two internally threaded glass barrels approximately 12.5 cm long of 1.5 cm internal diameter which are fused to a middle glass chamber of the same approximate dimensions. Addition of two fine-porosity sintered Pyrex frits gives rise to three independent chambers, the two end chambers of which will contain electrodes. The inner chamber serves as a liquid junction which helps to prevent the cross-contamination of products from the cathode and anode chambers. Unlike a standard H-type electrochemical cell, this middle chamber is placed near the bottom of the two electrode-containing chambers in order to help to minimize the amount of solvent needed. In some cases, all three chambers of the electrochemical cell are joined near the top using additional glass tubing. This allows for the equilibration of pressure among the chambers which sometimes builds up during the electrolyses. On the top of each chamber sits a Teflon® bushing which is held in place by a polymeric O-ring. These Teflon® bushings can be screwed tightly down to form a seal between the screw-thread tubing, the rubber O-ring and the electrode assembly. They serve to contain the inert atmosphere needed to preserve the anions that will be generated when the cell is in use and are needed to keep out atmospheric oxygen which would interfere with the process. Holes (of approximately 1.45 cm internal diameter) are present in the cathode and anode bushings to allow the individual electrode assemblies to fit cleanly through but are constricted enough to form a seal against the electrode assembly when tightened to the O-rings. The middle chamber is simply capped with a solid Teflon® plug (and rubber O-ring). All three chambers of the electrochemical cell are each filled with approximately 10 ml of concentrated ethylenediamine solutions of tetraalkylammonium salts. These salts serve as the supporting electrolyte (to carry charge) and are further present to be used as cations for the crystallization process. All the electrochemical cells are dried in an oven at 200 °C overnight before use in order to remove any moisture that would also interfere with the cathodic dissolution process.

4.3. Fabrication of the electrodes

The cathode electrodes are fabricated from the pure elements using the congruently melting binary telluride phase of a heavier main group element or post-transition metal. To make these electrodes, stoichiometric amounts of the pure elements (5–20 g of each) were heated to melt in a quartz container under a nitrogen atmosphere. Most melted easily, forming a shiny silver alloy-like plug in the bottom of the reaction vessel. The resulting regulus was stable under atmospheric conditions and could be cracked out of the reaction vessel and crushed to a fine powder on the benchtop using a mortar and pestle. The resulting powders were then checked by energy-dispersive spectroscopy (EDS) and X-ray powder diffraction for phase purity and recast into cylindrical electrodes of approximate 1 cm^2 surface area using pre-formed quartz electrode molds. The respective electrodes were broken out of their electrode molds and soldered to copper wires with standard Pb–Sn solder. They were then resealed into the remains of the original electrode mold (which now served as the electrode assembly) with epoxy to make them air tight. The electrode assemblies were then fitted into the Teflon® bushings of the appropriate electrode chamber and tightened into place for the electrolysis.

The anode electrodes were simply pieces of nickel foil (surface area, about 3–4 cm^2) which were similarly sealed into glass jackets with epoxy and fitted into the Teflon® bushings so as to be air tight. The preference for the use of nickel (over platinum) as a sacrificial electrode and its importance in the electrochemical process will be discussed later.

4.4. Purification of the solvent

The solvent of choice in these electrochemical experiments was in all cases ethylenediamine. This

solvent has been shown to be especially useful in the extraction studies of the alkali metal alloys of the heavier main group and post-transition elements which have resulted in the isolation of many Zintl compounds. The ethylenediamine was distilled under a nitrogen atmosphere first from CaH_2 and then from a red–brown solution of K_4Sn_9. Multiple distillations over K_4Sn_9 were typically required to obtain the purity of ethylenediamine needed in these experiments. The process for testing the purity of the solvent consisted of sampling the freshly distilled ethylenediamine by transferring an aliquot of it (5–10 ml) to a clean dry sample vial containing a few milligrams of K_4Sn_9, and then taking one drop of this solution and adding it to a second sample vial containing 10–20 ml of the same solvent. The purity of the ethylenediamine was determined by the length of time that this second sample stayed light red–brown in color, an extremely pure sample retaining its color for several days. This particular purity was determined to be suitable for the isolation of single-crystal telluride compounds, none of which showed any signs of decomposition in the solvent.

4.5. The choice of supporting electrolytes

The supporting electrolytes used in the electrochemical syntheses were tetraphenylphosphonium or tetraalkylammonium-based bromides or iodides obtained from Aldrich (97–99% purity) and were typically used without further purification. For those salts that were stable to temperatures of 150–200 °C, drying overnight in an oven at 150 °C was done to remove any possible moisture. The solubilities of these species in the ethylenediamine was very important as this directly affected the amount of current that could be passed through the cell. For the species used in the following syntheses, the general solubility trend was $(C_4H_9)_4N^+ \approx (C_6H_5)_4P^+ > (C_3H_7)_4N^+ > (C_2H_5)_4N^+ > (CH_3)_4N^+$. As will be shown later, the choice of supporting electrolyte greatly affected the products isolated, and simply changing it, sometimes only by one carbon atom, made the difference between isolating an isolated anion, a large anionic cluster, a one-dimensional chain material, or no crystals at all.

4.6 The cathode reaction

The cathodic dissolution reaction that produces Zintl anion clusters is shown in Fig. 1. In this figure, current, which is supplied by an external power supply (LakeShore Model 120CS variable-current supply, not shown), is applied to the cathode electrode causing alloy AB to dissolve into a stream of intensely colored anionic species. The stream originates from the cathode electrode and, as it is heavier than the

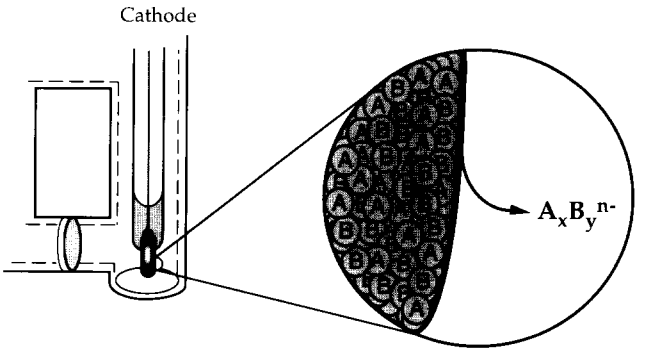

Fig. 1. The cathodic dissolution reaction that produces Zintl anion clusters. In the figure, the cathode alloy AB obtains electrons from an external power supply and dissolves to form anions $A_xB_y^{n-}$. These anions then crystallize in a concentrated supporting electrolyte of cations (C^+) to form single crystals of $C_n(A_xB_y)$ over time.

electrolyte material, immediately sinks to the bottom of the cathode chamber. On occasion, this stream has been observed to bend toward the direction of the anode chamber – an effect, no doubt, of the intense ion current present in all three chambers of the electrochemical cell. The color of these anion streams varies with both the electrode material and the supporting electrolyte and ranges in color from bright orange to deep purple depending on the reaction conditions. As the concentration of anions generated in these streams increases in a concentrated supporting electrolyte of cations, crystals form and deposit throughout the cathode chamber. These crystals have been observed growing on the bottom of the cathode chamber, in and around the glass frits, on pieces of the epoxy that invariably come off of the electrode assembly, on the glass shaft of the cathode assembly, and on the cathode electrode itself. The growth of crystals on the cathode electrode presents a problem in most cases as this results in the build-up of an insulating layer which prevents further dissolution of the electrode material. Such a build-up causes an inevitable reduction in the applicable current and ultimately terminates the reactions.

4.7. The anode reaction

As mentioned earlier, nickel is used as the sacrificial anode electrode in the electrochemical process. The use of nickel has been found to be clearly advantageous over platinum as it generates an insoluble purple precipitate in the anode chamber whereas platinum does not. Along with the use of the liquid junction, the generation of this solid in the anode chamber helps to prevent cross-contamination with the cathodic prod-

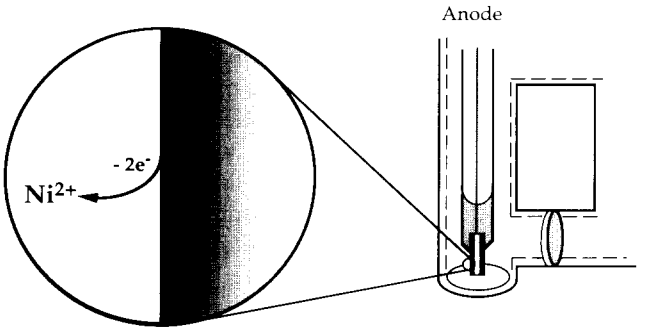

Fig. 2. The anode reaction. In this figure, the nickel plate dissolves into Ni^{2+} cations which can combine with the supporting electrolyte's counteranions (I^-) to form purple crystals of nominal composition "NiI_2".

ucts and subsequently allows the reactions to run for longer periods of time.

The anode reaction is shown in Fig. 2. In this reaction, the nickel plate loses electrons to the external power supply and generates Ni^{2+} cations in the anode chamber. These Ni^{2+} cations can then react with the counteranion of the tetraalkylammonium salt of the supporting electrolyte (Br^- or I^-). These reactions result in either the formation of a purple powder (when Br^- is the counteranion) or a purple crystalline material (when I^- is the counteranion). These purple crystals have in all cases been generated as extremely twinned samples that immediately lose solvent molecules when exposed to the atmosphere of the dry-box (as evidenced by their turning lighter shades of purple with time, eventually becoming cloudy looking, and then turning completely opaque after several hours). They have therefore only been incompletely characterized by EDS analysis. The EDS analysis of both the purple powder and the purple crystalline materials shows an Ni:Br (or I) ratio of exactly 1:2, giving rise to the formulations of $NiBr_2 \cdot x(en)$ or $NiI_2 \cdot x(en)$. Both materials have also been observed to be air sensitive.

4.8. Other experimental conditions

All the electrochemical reactions were run at room temperature on the benchtop under the contained inert He atmospheres (less than 1 ppm O_2) present within the chambers of the cells. All cells were loaded in the dry-box, tightly sealed and then brought out to be electrolyzed on the benchtop. Each electrochemical cell was hooked up to its own individual constant-current power supply which was connected to the leads of the cathode and anode electrodes and set to run at the maximum current allowed. This current range was determined by the solubility of the tetraalkylammonium salts in the ethylenediamine, and was typically 100 μA to 1 mA (with the maximum compliance voltage of the power supplies being equal to 11 V). The majority of these reactions were run for 2–5 days, although in some cases crystals large enough for single-crystal X-ray analysis were seen after only 24 h, while in others they were not large enough for some 10 days or more. Allowing the reactions to run for longer periods of time did, in general, increase the chemical yields but was limited by the build-up of insulating layers on the cathode electrode, the physical loss of this electrode (which on occasion fell off owing to its reduction in size, inadequate soldering to the copper wire or the erosion of the epoxy holding it in the electrode assembly), and the ever-present potential for cross-contamination from products generated in the anode chamber. Allowing the reactions to run for long periods of time did not, however, in general increase the electrochemical yields, especially when these insulating layers formed. This result, rather obviously, is due to the continuation of the passage of current without any further dissolution of the electrode material. This current could go into reducing the solvent, the electrolyte or other unrelated items.

5. Electrochemical synthesis of molecular species

5.1. Gold tellurides

Compounds containing gold and tellurium have been of interest recently as possible erasable laser recording media [18] and as indicators of the geochemical formation conditions of minerals [19]. However, the majority of publications in this field are concerned with the leaching of gold from $AuTe_2$ rather than compounds formed from it [20]. In the Au–Te phase diagram, the $AuTe_2$ phase is the only congruently melting gold telluride. Gold tellurides occur naturally in this $AuTe_2$ form as the minerals calaverite [21] and krennerite [22], as well as in an Au_2Te_3 form, the thermally metastable mineral montbrayite [23]. Gold–tellurium materials which contain halogens, such as AuTeI [24] and $AuTe_2X$(X = Cl, Br or I) [25], are also known. Several potassium gold telluride compounds also exist. These polyanions include $[KAu_9Te_7]^{4-}$ [2h], $[K_2Au_4Te_4(en)_4]^{2-}$ [2h] $[K_2Au_4Te_4(DMF)_2(CH_3OH)_2]^{2-}$ (DMF = dimethyl formamide) (which were formed from the extraction of alloy phases), as well as the solid state material KAuTe [26]. There are, however, apparently only three known examples of isolated Au–Te polyanions, which were found in the compounds $[\{(C_6H_5)_3P\}_2N]_2Au_2Te_4$ [2i], $[(C_2H_5)_4N]_3AuTe_7$ [27a] and $[(C_2H_5)_4N]_4Au_2Te_{12}$ [27b].

5.2. Synthesis and structure of $[C_4H_9)_4N]_3Au_3Te_4$

Single crystals of the gold telluride compound $[C_4H_9)_4N]_3Au_3Te_4$ (**1**) were prepared by cathodically dissolving an $AuTe_2$ alloy electrode in a 0.40 M solution of tetrabutylammonium iodide in ethylenediamine in the two-compartment liquid-junction air-tight electrochemical cell described above [28]. Application of a constant current of 300 μA immediately gave rise to a deep-brown stream of polyanions which surrounded the $AuTe_2$ cathode and then slowly sank to the bottom of the cathode chamber. After 2 days, dark-brown, rectangularly shaped crystals were isolated from the cathode chamber in greater than 60% yield (electrochemical yield, 26%). These crystals were found growing on the $AuTe_2$ cathode and throughout the cathode chamber. EDS analysis of several of these crystals showed an Au:Te ratio of between 1:1.29 and 1:1.43. A control experiment of powdered $AuTe_2$ and $(C_4H_9)_4NI$ in ethylenediamine did not give rise to any color (no polyanions), and varying the current from 100 μA to 1 mA had no effect on the product, yielding the dark-brown rectangular crystals in all cases.

The X-ray structural analysis of a single dark-brown, rectangularly shaped crystal of $[C_4H_9)_4N]_3Au_3Te_4$ (**1**) revealed the novel $Au_3Te_4^{3-}$ anion which is shown in Fig. 3. There are two slightly puckered, crystallographically independent $Au_3Te_4^{3-}$ anions in the unit cell, each possessing crystallographic two-fold symmetry in the solid state. The central Au atom in a given $Au_3Te_4^{3-}$ anion resides on the Wyckoff 4e special position in space group $C2/c$, lying on a c glide plane. Each $Au_3Te_4^{3-}$ anion contains three Au(I) atoms joined together by Au–Au bonds of 3.049(3) Å or 3.015(3) Å making an Au–Au–Au angle of 78.4(1)° or 81.1(1)° respectively. These Au–Au distances are somewhat longer than the 2.88 Å Au–Au distances observed in gold metal [24]. The transannular nonbonded Au–Au distance is either 3.854(4) or 3.922(4) Å. Although it cannot easily be seen in Fig. 3, the $Au_3Te_4^{3-}$ anion is not planar, with the linear Te(1)–Au(2)–Te(2) and equivalent Te(1*)–Au(2*)–Te(2*) units rotated approximately 9° out of the molecular Au(2)–Au(1)–Au(2*) best planes.

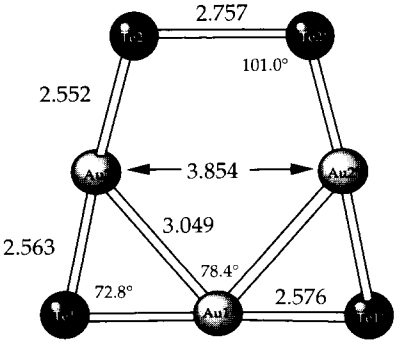

Fig. 3. The structure of one of the two crystallographically independent $Au_3Te_4^{3-}$ Zintl anions produced by the cathodic dissolution of an $AuTe_2$ alloy electrode in a tetrabutylammonium iodide supporting electrolyte.

The oxidation state of Au(I) is firmly established in this compound by two independent observations: (1) the linear arrangement about the Au center, a common coordination environment for Au(I) but a rare one for Au(II) and an unknown one for Au(III); (2) the Au–Au distances which are comparable with those in the other structurally characterized Au(I) compounds. As expected for Au(I), the Te–Au–Te angles in the $[C_4H_9)_4N]_3Au_3Te_4$ (**1**) compound are all close to 180°, varying from 172.5(2)° to 178.9(1)°. Au–Te bonds range from 2.549(4) to 2.589(3) Å, and the Te–Te distances of 2.757(8) and 2.760(7) Å are similar to the Te–Te distances observed in other structurally characterized tellurides.

The charge of 3− on the $Au_3Te_4^{3-}$ anion is firmly established by the presence of two of these crystallographically independent anions in the unit cell, each of which lies on a twofold axis. Because of this arrangement, only half of each of the two $Au_3Te_4^{3-}$ anions is present in the asymmetric unit (1.5− × 2 = 3− total charge). There are also four crystallographically independent tetrabutylammonium cations present in the asymmetric unit (two of which are located at general positions in the lattice, and two of which sit on sites of crystallographic twofold symmetry).

The full unit cell of $[C_4H_9)_4N]_3Au_3Te_4$ contains 24 $[C_4H_9)_4N]^+$ cations, three for each of the eight $[Au_3Te_4]^{3-}$ anions also present there ($Z = 8$). These $[C_4H_9)_4N]^+$ cations completely surround the $Au_3Te_4^{3-}$ anions in the solid state. Not surprisingly, this geometry results in the observed fact that the dark-brown crystals of this compound are extremely soft and can be easily smeared out on a piece of filter paper. Also, given this arrangement, $[C_4H_9)_4N]_3Au_3Te_4$ (**1**) is expected to be an insulator.

5.3. Antimony tellurides

In sharp contrast with the numerous examples of antimony sulfides (see for example [29]) and selenides (see for example [30]) there are very few examples of antimony telluride compounds in the literature. Apart from the known binary (and congruently melting) phase Sb_2Te_3 [31], there appears to be only four known antimony telluride polyanion structures: $BaSbTe_3$ [32], $LiSbTe_2$ [33a], K_3SbTe_3 [33b] and $AgSbTe_2$ [34]. All these compounds have been prepared by the high temperature fusion of the elements and are extremely air sensitive. There also exist several mixed antimony germanium telluride com-

pounds such as $GeSb_4Te_7$ [35], $GeSb_2Te_4$ [35] and $Ge_2Sb_2Te_5$ [35] which are stable under atmospheric conditions and have been studied for their potential semiconducting properties. These three compounds have also been prepared by the high temperature fusion of the elements.

The electrochemically controlled cathodic dissolution of Sb_2Te_3 electrodes in ethylenediamine solutions of tetraalkylammonium supporting electrolytes has resulted in the production of five new compounds (containing four new anions) which have not been previously prepared by any other high temperature fusion of extraction method. When considering the synthesis of these materials, one must note that antimony and tellurium are adjacent to one another in the periodic table and, as a result, X-ray crystallography cannot be used to identify the products completely. This may be one of the reasons that those who work with the high temperature fusion and extraction techniques have, in general, avoided this system. Characterization of the compounds formed from this system has relied on a combination of X-ray crystallography, EDS analysis, comparison with other known antimony and tellurium bond lengths and angles, and on the chemically reasonable connectivities expected for antimony and tellurium.

5.4. Synthesis and structures of $[(CH_3)_4N]_4Sb_2Te_5$ and $[(C_2H_5)_4N]_4Sb_2Te_5$

Single crystals of the antimony telluride compounds $[(CH_3)_4N]_4Sb_2Te_5$ (**2**) and $[(C_2H_5)_4N]_4Sb_2Te_5$ (**3**) were prepared using the electrochemical synthetic method described above by cathodically dissolving Sb_2Te_3 alloy electrodes which were made by melting stoichiometric amounts of the elements to produce this congruently melting phase [36]. The electrochemical cell (described above) was filled with either a solution of 0.15 M tetramethylammonium iodide in ethylenediamine for the synthesis of $[(CH_3)_4N]_4Sb_2Te_5$ (**2**), or a 0.30 M solution of tetraethylammonium iodide in ethylenediamine for the synthesis of $[(C_2H_5)_4N]_4Sb_2Te_5$ (**3**). For the synthesis of $[(CH_3)_4N]_4Sb_2Te_5$ (**2**), application of a current of 100 μA to the Sb_2Te_3 cathode resulted in the production of a faint light-brown stream of anions which completely surrounded it and then sank to the bottom of the cathode chamber. The low solubility of tetramethylammonium iodide in ethylenediamine limited the initial current to a maximum of 100 μA which decreased over time as an insulating brown crystalline layer (the elemental microprobe analysis of which showed an Sb:Te ratio of 1:2.48) formed on the Sb_2Te_3 cathode. Although single crystals were seen in the cathode chamber after only 5 days, they did not seem large enough for single-crystal X-ray analysis, and the reaction was allowed to continue for 5 more days. After a total of 10 days, a current of less than 1 μA was able to pass through the cell, and the reaction was terminated. Upon isolation, dark-brown hexagonal plate crystals (having an EDS ratio of Sb:Te = 1:2.45 to 1:2.62) of the antimony telluride Zintl compound $[(CH_3)_4N]_4Sb_2Te_5$ (**2**) were found growing on the Sb_2Te_3 cathode and throughout the cathode chamber. These crystals, however, were isolated with a low yield (6%), presumably because of the formation of this insulating layer which prevented further dissolution of the Sb_2Te_3 cathode.

When the supporting electrolyte was changed to a 0.30 M ethylenediamine solution of tetraethylammonium iodide, an initial current of 300 μA could be applied. This resulted in the generation of a deep-red–brown stream of anions which completely surrounded the Sb_2Te_3 cathode and then slowly sank to the bottom of the cathode chamber. After approximately 5 days, the dissolution reaction resulted in the formation of dark-brown diamond-shaped crystals of $[(C_2H_5)_4N]_4Sb_2Te_5$ (**3**) which were found growing on the Sb_2Te_3 cathode and throughout the cathode chamber. Although these crystals also grow on the electrode surface, they have been observed to be considerably larger than those formed from the reaction in tetramethylammonium iodide and tend to fall off of the cathode surface, allowing sections of it to remain exposed and continue to dissolve. No reductions in current occurred over the 5 day period. The chemical and electrochemical yields for these crystals were 17% and 33%. The EDS Sb:Te ratio in these crystals was essentially the same as for $[(CH_3)_4N]_4Sb_2Te_5$ (**2**), varying from 1:2.42 to 1:2.65.

Single-crystal X-ray analysis of the brown hexagonal plate crystals formed from the cathodic dissolution of Sb_2Te_3 in tetramethylammonium iodide revealed the compound $[(CH_3)_4N]_4Sb_2Te_5$ (**2**) which crystallizes in the space group $P2_1/c$ with four independent $Sb_2Te_5^{4-}$ anions in the unit cell. The structure of the $Sb_2Te_5^{4-}$ anion formed from this reaction is shown in Fig. 4(A). The anion consists of two distorted $SbTe_3$ trigonal pyramids that share a corner Te atom making an Sb–Te–Sb angle of 87.4(2)°C. Although it appears highly symmetric, the anion displays only approximate *2mm* point group symmetry in the solid state. The geometry of the Sb in the $Sb_2Te_5^{4-}$ anion is similar to that observed in the Zintl phase compound K_3SbTe_3 [33b], which consists of discrete $SbTe_3^{3-}$ trigonal pyramids. This latter compound has three equivalent Te–Sb–Te bond angles of 101.86(2)° and Sb–Te bond distances of 2.7831(7) Å. In **2**, terminal Sb–Te bond distances range from 2.695(7) to 2.758(6) Å with internal Sb–Te bond distances of 2.779(6) and 2.816(7) Å. Angles within the $SbTe_3$ pyramids are

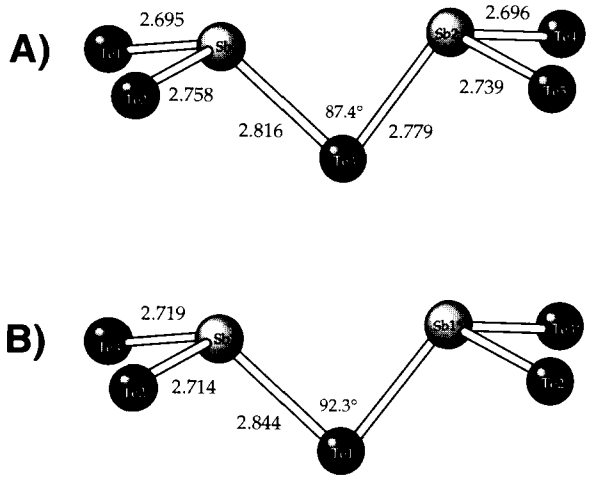

Fig. 4. (A) The structure of the $Sb_2Te_5^{4-}$ Zintl anion produced by the cathodic dissolution reaction of an Sb_2Te_3 alloy electrode in a tetramethylammonium iodide supporting electrolyte. (B) The structure of the $Sb_2Te_5^{4-}$ Zintl anion produced by the cathodic dissolution reaction of an Sb_2Te_3 alloy electrode in a tetraethylammonium iodide supporting electrolyte.

more obtuse than those in K_3SbTe_3, ranging from 102.0(2) to 107.8(2)°.

The charge of 4− on the $Sb_2Te_5^{4-}$ anion is firmly established by the presence of four crystallographically independent tetramethylammonium cations in the asymmetric unit. Each of the carbon and nitrogen atoms in these tetramethylammonium cations is located at general position in the lattice. Since $Z = 4$, there are four complete $Sb_2Te_5^{4-}$ anions and 16 tetramethylammonium cations in the full unit cell.

Assignment of Sb and Te atoms in this anion was based on their chemically reasonable connectivities and multiple EDS ratios whose average was 1:2.53. This assignment is reasonable, and accounts for both the observed bond distances and angles and also the observed charge of 4− on the anion. The complete structure of $[(CH_3)_4N]_4Sb_2Te_5$ (**2**) contains isolated $Sb_2Te_5^{4-}$ anions which are completely surrounded by tetramethylammonium cations in the solid state. The nearest distances between adjacent $Sb_2Te_5^{4-}$ anions ranges between 6.253 and 7.390 Å. These distances preclude the possibility of any possible interactions between the anions and suggest that $[(CH_3)_4N]_4Sb_2Te_5$ (**2**) is an insulator.

The structure of the $Sb_2Te_5^{4-}$ anion produced from the cathodic dissolution of an Sb_2Te_3 alloy electrode in a $(C_2H_5)_4N^+$ supporting electrolyte is shown in Fig. 4(B). The structure of this anion is essentially the same as that produced from the electrolysis in $(CH_3)_4N^+$, with some slight variations in bond lengths and angles. For instance, the internal Sb–Te bond distances in **2** are inequivalent (2.816(7) and 2.779(6) Å) whereas those in **3** are exactly the same (2.844(3) Å). There are also two shorter (2.696(7) and 2.695(7) Å) and two longer (2.758(6) and 2.739(7) Å) terminal Sb–Te bonds in **2**, whereas both terminal Sb–Te bonds in **3** are almost exactly the same (2.719(4) and 2.714(4) Å). The Sb–Te–Sb angle of 87.4(2)° in **2** is also more acute than in **3** where it is observed to be 92.3(1)°.

In the structure of the $(C_2H_5)_4N^+$ salt (**3**), the central Te atom of the $Sb_2Te_5^{4-}$ anion, Te(1), lies on the Wyckoff 4a special position and has *m* symmetry. In the asymmetric unit, only half of the $Sb_2Te_5^{4-}$ anion is present, together with one complete tetraethylammonium cation and two cations that lie on 2-fold special positions. Thus the charge on the $Sb_2Te_5^{4-}$ anion is also confirmed to be 4− in this salt. As in **2**, the complete structure of $[(C_2H_5)_4N]_4Sb_2Te_5$ (**3**) consists of $Sb_2Te_5^{4-}$ anions which are completely surrounded by tetraethylammonium cations.

5.5. Synthesis and structure of $[(C_2H_5)_4N]_4Sb_6Te_9 \cdot (0.5en)$

Single crystals of the compound $[(C_2H_5)_4N]_4Sb_6Te_9 \cdot (0.5en)$ (**4**) were prepared concurrently with $[(C_2H_5)_4N]_4Sb_2Te_5$ (**3**) from the cathodic dissolution of an Sb_2Te_3 alloy cathode in a tetraethylammonium supporting electrolyte [36]. After a total of 5 days, the electrolysis resulted in the formation of these two solid products which were separated by eye, based on their different morphologies. They were isolated in an approximate 90:10 ratio (favoring $(C_2H_5)_4N]_4Sb_2Te_5$ (**3**)). It is unknown which compound forms first, or whether they both form at the same time, but independent experiments suggest that one is not interconverted into the other on standing in the electrolyte solution. These two compounds appear to be the only solid products obtained from the cathodic dissolution process in the tetraethylammonium supporting electrolyte and are not obtained from a control experiment of powdered Sb_2Te_3 and $(C_2H_5)_4NI$ in ethylenediamine. The chemical and electrochemical yields for $[(C_2H_5)_4N]_4Sb_6Te_9 \cdot (0.5en)$ (**4**) were rather modest, 3% and 2% respectively.

Single-crystal X-ray analysis of the dark-brown prismatic crystals of $[(C_2H_5)_4N]_4Sb_6Te_9 \cdot (0.5en)$ (**4**) revealed the novel antimony telluride anion $Sb_6Te_9^{4-}$ (which can be seen in Fig. 5). The compound crystallizes in the space group $P2_1/n$ with one crystallographically independent $Sb_6Te_9^{4-}$ anion, four complete tetraethylammonium cations and half an ethylenediamine molecule in the asymmetric unit. Some of the bond distances and angles present in the $Sb_6Te_9^{4-}$ anion are shown in Fig. 5. This anion, like the two $Sb_2Te_5^{4-}$ antimony telluride anions, displays approximate, but not crystallographically imposed, 2*mm* point group symmetry in the solid state.

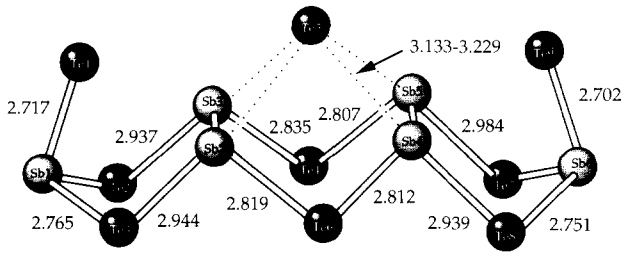

Fig. 5. The structure of the $Sb_6Te_9^{4-}$ Zintl anion produced by the cathodic dissolution of an Sb_2Te_3 alloy electrode in a tetraethylammonium iodide supporting electrolyte. The Sb–Te interactions involving Te(5) are as follows: Sb(2)–Te5, 3.179(5) Å; Sb(3)–Te(5), 3.188(5) Å; Sb(4)–Te(5), 3.229(5) Å; Sb(5)–Te(5) = 3.133(5) Å. The Sb–Sb bond distances are 2.814(5) Å for Sb(2)–Sb(3), and 2.841(5) Å for Sb(4)–Sb(5).

The assignment of Sb and Te atoms in the $Sb_6Te_9^{4-}$ anion was based on their chemically reasonable connectivities and multiple elemental microprobe analyses on different crystals which yielded Sb:Te ratios of 1:1.45 to 1:1.52. The overall charge of 4− on the anion was established by the presence of four crystallographically independent tetraethylammonium cations per anion in the asymmetric unit. The distribution of charge in this unusual 15-membered antimony telluride Zintl anion can be rationalized in the following manner: Terminal tellurium atoms Te(1) and Te(9), each having only one bond, have an expected charge of 1−. The capped Te(5) atom, which is weakly coordinated to antimony atoms Sb(2)–Sb(5), exists as a dianion (2− charge). All the other Te atoms in the anion are two-coordinate and, together with all the antimony atoms in the anion which are three-coordinate, have no charge. Another equally valid way of looking at the bonding in the $Sb_6Te_9^{4-}$ anion would be to adopt an ionic model which would assume that the two Sb dimers (each containing a homonuclear Sb–Sb bond) in the anion each have a charge of 4+, and that the two isolated Sb atoms, Sb(1) and Sb(6), are present as 3+. All the Te atoms must then have a formal 2− charge, including the capped Te(5) atom.

The unusual capped four-coordination environment of tellurium found in the $Sb_6Te_9^{4-}$ anion (Te(5)) has been seen in the solid state chalcogenide compound $K_4Cu_8Te_{11}$ [37] but is unprecedented in antimony tellurides. This geometry results in unusually long Sb–Te interactions of between 3.133(5) and 3.229(5) Å, which are longer than any previously reported Sb–Te bond (and as such, are drawn as dotted lines in Fig. 5). It is very unlikely that four two-electron bonds actually exist in the $Sb_6Te_9^{4-}$ anion and is more likely that the Te(5) atom is simply shared equally among the four Sb atoms in the ring, being held in place by weak bonding contributions from all four Sb atoms. The other Sb–Te bond distances of 2.702(5) and 2.717(5) Å for the two terminal Sb–Te bonds, and 2.765(6)–2.984(5) Å for internal Sb–Te bonds, as well as the Sb–Sb bond distances of 2.841(5) and 2.841(5) Å in this anion are all within the values expected for these interactions.

5.6 Synthesis and structures of $[(C_3H_7)_4N]_4Sb_4Te_4$ and $[(C_3H_7)_4N]_3Sb_9Te_6$

Using the same Sb_2Te_3 alloy electrodes mentioned above, but this time changing the supporting electrolyte to a 0.56 M solution of tetrapropylammonium bromide in ethylenediamine, single crystals of the antimony tellurides $[(C_3H_7)_4N]_4Sb_4Te_4$ (**5**) and $[(C_3H_7)_4N]_3Sb_9Te_6$ (**6**) were obtained [38]. The cathodic dissolution reaction of the Sb_2Te_3 alloy electrode in the 0.56 M tetrapropylammonium bromide solution of ethylenediamine running at a current density of about 300 $\mu A\ cm^{-2}$, immediately gave rise to a deep-brown stream of anions which surrounded the cathode and then slowly sank to the bottom of the cathode chamber. After only 1 day, a red–brown crystalline solid, which was later identified as $[(C_3H_7)_4N]_4Sb_4Te_4$ (**5**) was observed growing on the Sb_2Te_3 cathode. After approximately 2 days, the deep-brown catholyte solution also yielded brown spear-shaped crystals of $[(C_3H_7)_4N]_3Sb_9Te_6$ (**6**) which were found growing mainly on the bottom of the chamber. The reaction was isolated after 5 days yielding $[(C_3H_7)_4N]_4Sb_4Te_4$ (**5**) and $[(C_3H_7)_4N]_3Sb_9Te_6$ (**6**) in an approximate 80:20 ratio. Chemical and electrochemical yields, as calculated on the basis of moles of Sb, were 29% and 17% for **5** and 12% and 2% for **6**. These two compounds appeared to be the only solid products of the electrochemical dissolution reaction and were not obtained from control experiments of powdered Sb_2Te_3 and $(C_3H_7)_4NBr$ in ethylenediamine. Independent experiments have also shown that $[(C_3H_7)_4N]_4Sb_4Te_4$ (**5**) is not converted into $[(C_3H_7)_4N]_3Sb_9Te_6$ (**6**) on standing in the electrolyte solution which suggests that the two anions are formed independently by the dissolution process.

The antimony telluride Zintl compound $[(C_3H_7)_4N]_4Sb_4Te_4$ (**5**) crystallizes in space group *Pbcn* (No. 60) with eight $Sb_4Te_4^{4-}$ anions and 32 tetrapropylammonium cations in the unit cell ($Z = 8$). The structure of the $Sb_4Te_4^{4-}$ anion is shown in Fig. 6. The anion consists of a folded Sb_4 ring to which four terminal Te atoms are attached in the equatorial positions. The anion displays approximate but not crystallographically imposed *2mm* point group symmetry in the sold state. This geometry is quite different from the bare Sb_4^{2-} anion which exists as a square planar moiety [39] but more closely resembles that of the compound (*tert* $C_4H_9)_4Sb_4$ which has *tert*-butyl groups bonded to a folded Sb_4 ring in equatorial positions [40]. The Sb–Sb distances in the $Sb_4Te_4^{4-}$

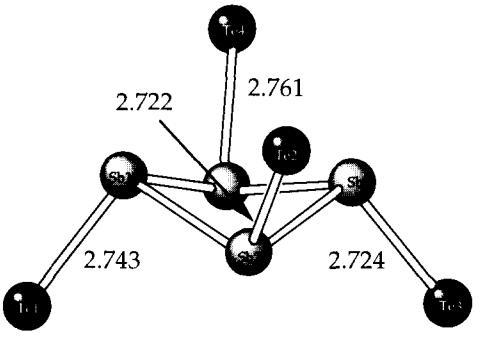

Fig. 6. The structure of the $Sb_4Te_4^{4-}$ Zintl anion produced by the cathodic dissolution of an Sb_2Te_3 alloy electrode in a tetrapropylammonium bromide supporting electrolyte. The anion forms a puckered Sb_4 square with Sb–Sb distances as follows: Sb(1)–Sb(2), 2.883(4) Å; Sb(2)–Sb(3), 2.849(4) Å; Sb(3)–Sb(4), 2.836(4) Å; Sb(4)–Sb(1), 2.864(4) Å. The transannular non-bonded Sb–Sb distances are 3.911(3) Å for Sb(1)–Sb(3) and 3.921(4) Å for Sb(2)–Sb(4).

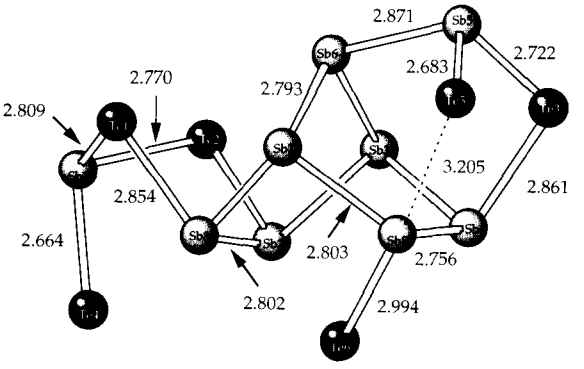

Fig. 7. The structure of the $Sb_9Te_6^{3-}$ Zintl anion produced by the cathodic dissolution of an Sb_2Te_3 alloy electrode in a tetrapropylammonium bromide supporting electrolyte. The dotted line represents a long Sb–Te contact of 3.205(6) Å. Some other Sb–Sb and Sb–Te bond distances and angles are noted.

anion are in the range 2.836(4)–2.883(4) Å and can be compared with those in the *tert*-$(C_4H_9)_4Sb_4$ compound which fall in the range 2.814(2)–2.821(2) Å. The average transannular non-bonded Sb–Sb distance in the $Sb_4Te_4^{4-}$ anion is 3.913 Å. For comparison, the average Sb–Sb distance in the Sb_4^{2-} anion is 2.750 Å, and it has an average transannular non-bonded Sb–Sb distance of 3.889Å. The Sb–Te bond distances in the $Sb_4Te_4^{4-}$ anion are in the range 2.722(4)–2.761(4) Å. Paucity of structurally characterized Sb–Te compounds makes extensive comparisons with these Sb–Te bond distances difficult, but they are consistent with the other Sb–Te Zintl anions reported in this article. For other comparisons, the ternary Zintl phase compound K_3SbTe_3 (mentioned earlier) consists of discrete trigonal pyramidal anionic units having three equivalent terminal Sb–Te bond distances of 2.7831(7) Å [33b]. The Sb–Te bond distance in the solid state phase Sb_2Te_3 is 2.974 Å, and Sb–Te distances in $BaSbTe_3$ are in the range 2.832–3.090 Å [32]. The unit cell of **5** contains eight $Sb_4Te_4^{4-}$ anions and 32 tetrapropylammonium cations in the solid state. As in all the structures mentioned thus far, these tetrapropylammonium cations completely surround the $Sb_4Te_4^{4-}$ anions giving rise to what is most probably another insulating material that is not expected to have any interesting conductive properties.

The antimony telluride $[(C_3H_7)_4N]_3Sb_9Te_6$ (**6**) crystallizes in monoclinic space group $P2_1/c$ with four $Sb_9Te_6^{3-}$ anions in the unit cell. The structure of the $Sb_9Te_6^{3-}$ anion is shown in Fig. 7. The assignment of Sb and Te atoms in this anion was based on their chemically reasonable connectivities and an elemental microprobe analysis which yielded an Sb:Te ratio of 1.5:1. In describing the structure of the $Sb_9Te_6^{3-}$ anion, one can think of it as the fusion of two well-known structure types (Scheme 1): an Sb_6Te_2 cage (**a**) that resembles those found in X_4N_4 (X = As, S or Se), [41–43], X_4S_4(X = P or Te) [44,45] and As_4Se_4 [46] and a bicyclic Sb_6Te_2 moiety (**b**) with an Sb–Sb transannular closure and a geometry closely resembling that of Se_8^{2+} [47].

An interesting feature of the structure of $Sb_9Te_6^{3-}$ is the pseudo-four-coordinated Sb(9) atom which is bonded to Sb(4) and Sb(7) atoms at 2.756(5) Å and 2.803(5) Å, but displays an abnormally long Sb(9)–Te(6) contact of 2.994(5) Å. The other two Sb–terminal Te contacts in the anion are much shorter with Sb(5)–Te(5) at 2.683(6) Å and Sb(1)–Te(4) at 2.664(5) Å. The lengthening of the terminal Sb(9)–Te(6) contact is most probably due to the weak coordination of Sb(9) to Te(5) at 3.205(6) Å, making Sb(9) pseudo four-coordinate. It is interesting to note that all three of the terminal Sb–Te bonds are "*endo*" relative to the cluster. It is not clear whether this is simply due to packing forces in the crystal or whether the effect is driven by weak Sb–Te interactions such as those involving Te(4) and Sb(2) or Sb(8) at 3.712(5) and 3.665(5) Å or Te(6) and Sb(4) at 3.317(6) Å. The Sb–Sb distances in $Sb_9Te_6^{3-}$ are in the range 2.756(5)–2.871(5) Å and internal Sb–Te distances vary from 2.722(7) to 2.878(5) Å, all of which are comparable with those in the other tetrapropylammonium salt (containing the $Sb_4Te_4^{4-}$ anion) and in the other structurally characterized antimony tellurides. Although this structure is just another example of a

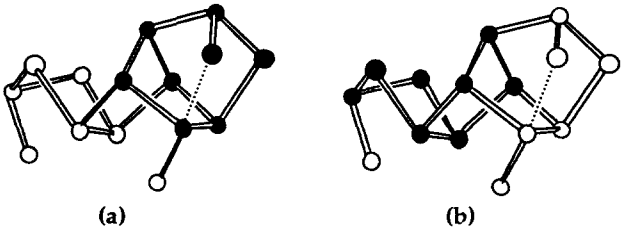

Scheme 1.

highly charged Zintl anion which is completely isolated (and should therefore not have any interesting conductive properties), it does illustrate the unusual structural compositions that can be made from the antimony telluride system. Two 15-membered clusters have been isolated from this system, both impossible to predict from the simple Sb_2Te_3 starting electrode material.

5.7. Zintl anions from the arsenic and tin telluride systems

The binary compounds formed between the chalcogenides and the pnictides range from molecules to three-dimensional solids. The properties of the lighter members of this class, such as the minerals orpiment (As_2S_3) [48] and realgar (As_4S_4) [49], resemble those of molecular materials, while the heavier solids, such as the mineral tellurobismuthite (Bi_2Te_3), have interesting optical and electronic properties [50]. Many of these M_2X_3 solids adopt the rhombohedral $R\bar{3}m$ tetradymite structure type. It is also possible to solubilize binary anionic clusters from neutral solids containing the group 15 and 16 elements as exemplified by the formation of As–S polyanions by the treatment of arsenic sulfides with organic amines [51] and the work of Sheldrick and coworkers [52] involving solventothermal reactions of arsenic sulfides and selenides with carbonates in methanol. Other arsenic selenide compounds have been isolated by Kolis and coworkers [53]. In the As–Te Zintl polyanion system, the clusters $As_{10}Te_3^{2-}$ [54], $As_{11}Te^{3-}$ [55], $As_2Te_6^{2-}$ [56] and $As_4Te_6^{4-}$ [57] are known. All these anions have been synthesized through the ethylenediamine extraction of alkali metal arsenic telluride alloys.

Moving over to the tin telluride system, very little work seems to have been done. In fact, when compared with the binary and ternary main group oxides (such as SiO_2), the heavier main group chalcogenides of group 13 have received little attention. As expected by analogy to silicate chemistry, the structures of the known compounds in this system are based on tetrahedral building blocks. Examples such as $Ge_2S_{16}^{4-}$ [58], $Ge_4S_{10}^{4-}$, [59], $GeSe_4^{4-}$ [60], $Ge_2Se_6^{4-}$ [6], SnS_4^{4-} [62], $Sn_2S_6^{4-}$ [63] and $Sn_2Se_6^{4-}$ [64] have been isolated. Several group 13 telluride Zintl anions are also known. They include $Si_4Te_{10}^{4-}$ [65], $GeTe_2^{1-}$ [66]. $GeTe_4^{2-}$ [67], $Ge_4Te_{10}^{4-}$ [68a], $Ge_4Te_{10}^{8-}$ [68b], $SnTe_4^{4-}$ [69], $SnTe_5^{2-}$ [70], $Sn_2Te_6^{4-}$ [71] and $Sn_2Te_7^{6-}$ [72]. The majority of these compounds have been prepared through the high temperature fusion and/or extraction techniques, although some have been made by Krebs et al. by the treatment of the binary main group sulfides or selenides with HX^- or X^{2-} (X = S or Se) in aqueous solution.

The Zintl anions $As_2Te_6^{2-}$, $As_4Te_6^{4}$, $As_{10}Te_3^{2-}$, $Ge_4Te_{10}^{4-}$, $Sn_2Te_3^{2-}$ and $Sn_2Te_6^{4-}$ have all been produced by the electrochemical synthetic method described above, through a combination of varying the composition of the cathode electrode and through the choice of tetraalkylammonium halide supporting electrolytes [10]. As the structures of these anions are not new, they will not be discussed here. However, the mere synthesis of these molecular species illustrates the versatility of the synthetic technique, which has now been used successfully for many congruently melting main group telluride electrodes.

6. Electrochemical synthesis of one-dimensional chain materials

One-dimensional inorganic polymers are not rare. In fact, there are a reasonably large number of examples of these solids in the literature, especially in the main group oxides. Some examples of these one-dimensional main group oxide materials include SeO_2, Sb_2O_3 and HgO, as well as the chain silicate materials such as those of the pyroxene group [73]. There are far fewer examples of low dimensional materials in the corresponding heavier chalogenides. Some examples for sulfur include the infinite one-dimensional chain compounds SiS_2 [74] and $KFeS_2$ [75], which are made up of infinite chains of tetrahedra (containing either Si(IV) or Fe(III)) that share opposite edges. For selenium, the low dimensional compounds TlSe [76], $NaAlSe_2$ [77] and $TlAlSe_2$ [78] are known. In the tellurium system, compounds of the form $AMTe_2$, where A = Na or K and M = Al, Ga or In, have been prepared and structurally characterized [79]. The new mixed-metal one-dimensional mercury tin telluride polymer $HgSnTe_4^{2-}$ has also just recently been isolated [80]. This compound has been made both by the high temperature fusion of the elements and via the solventothermal reaction of K_4SnTe_4 with $HgCl_2$ in ethylenediamine at 100 °C.

Low dimensional inorganic materials are of interest because of the variety of anisotropic electrical, optical and magnetic properties that they may possess [81]. The class of polychalcogenide compounds, especially those containing multiple chalcogen–chalcogen bonds, are noteworthy here, as many have been used in commercially viable industrial processes. For example, polysulfide ligands have been of extensive use in the hydrosulfurization of oil and are thought to be present at the surface of metal sulfide catalysts [82]. Polychalcogenide glasses are also an important class of materials and have been shown to be useful as nonlinear optical materials, in photoconductive devices, as optical switches, and as media for optical information storage [83].

It has been shown that polychalcogenide ligands are more likely to be incorporated into solid state low dimensional lattices if low temperatures (below 500 °C) are used [84]. This is because of the thermal instability of the polychalcogenide fragments, which increases with increasing length, leading to the isolation of smaller and smaller fragments. The electrochemical synthetic technique presented herein is done at room temperature and thus should be amenable to producing low dimensional materials. This section will show how this is accomplished.

6.1. Synthesis and structure of $[(C_6H_5)_4P]GaTe_2(en)_2$

There are very few examples of compounds of gallium and the heavier group 16 elements in the literature. While the binary compounds GaTe, Ga_2Te_3 and Ga_2Te_5 have been known for a long time, most of the recent interest in this area has been directed toward the organometallic compounds of gallium with group 15 elements. Compounds such as $R_3Ga \cdot XR'_3$ (X = N, P or As) [85] and $(R_2Ga\text{–}XR'_2)_2$ (X = P or As) [86] for example, are of current interest as possible precursors to thin films of III–V materials [87]. The first example of a compound containing a Ga–Te bond was reported by Coates [88] in the adduct formed from the reaction of $Ga(CH_3)_3$ with $Te(CH_3)_2$. Since then, the compounds $\{[(CH_3)_3CCH_2]_2GaTe(C_6H_5)\}_2$, which was prepared from the reaction of $Ga[CH_2C(CH_3)_3]_2Cl$ with $LiTe(C_6H_5)$ in $(C_2H_5)_2O$ [89] and $\{(tert\text{-}C_4H_9)_2Ga[\mu\text{-}Te(tert\text{-}C_4H_9)]\}_2$, which was prepared by the ambient temperature reaction of $Ga(tert\text{-}C_4H_9)_3$ with metallic tellurium [90] appear to be the only examples of Ga–Te compounds with organic ligands. Isolated Ga–Te anions are even rarer with $K_6Ga_2Te_6$ prepared by the high temperature fusion of the elements [91] apparently being the only known example. Related work in the semiconductor industries has produced the compounds $XGaTe_2$ (X = Cu, Ag, In or Tl) [92] XGa_2Te_4 (X = Cd or Hg) [93a, b] and $Ag_2Ga_6Te_{10}$ [94] which have been studied for their optical, thermal and electrophysical properties.

The electrochemically controlled cathodic dissolution of telluride electrodes, which worked so well in the synthesis of Zintl anion clusters (Section 5), is used here in the gallium telluride system for the synthesis of $[(C_6H_5)_4P]GaTe_2(en)_2$ (**7**)—a new pseudo-one-dimensional gallium telluride [95]. This compound cannot be formally considered a Zintl compound as it contains ethylenediamine molecules which are directly bonded to the central gallium atom. It is also not exactly a one-dimensional material, as no direct bonds exist connecting it into such a structure (hydrogen bonding is responsible for the pseudo-one-dimensional nature of the material). Nevertheless, $[(C_6H_5)_4P]GaTe_2(en)_2$ (**7**) represents a new addition to the field of gallium tellurides and helps to demonstrate the versatility of the cathodic dissolution technique.

The cathodic dissolution reaction that produces the compound $[(C_6H_5)_4P]GaTe_2(en)_2$ (**7**) required the use of a Ga_2Te_3 cathode which was made by melting stoichiometric amounts of the elements under nitrogen in a quartz tube. Unlike the previous syntheses of these telluride alloys which melt easily with no obvious difficulties or dangers, the fusion reaction of Ga and Te is extremely violent, erupting in bright orange flames and leaving a shiny black solid as a final product. Precautions such as the reaction being done in a fume hood equipped with a fire extinguishing device, and the use of a safety shield and/or safety face shield should be initiated before attempting this synthesis. Once formed, the black solid is easily crushed into a fine powder and recast into cylindrical electrodes of approximately 1 cm^2 surface area. The recasting process is not accompanied with any violent reactions.

The synthesis of single crystals of $[(C_6H_5)_4P]GaTe_2(en)_2$ (**7**) was accomplished from the cathodic dissolution reaction of a Ga_2Te_3 electrode in a 0.5 M tetraphenylphosphonium bromide solution in ethylenediamine. The electrolysis took place in a two-compartment liquid-junction air-tight electrochemical cell equipped with a nickel plate counterelectrode. Each compartment of the electrochemical cell was filled with 10 ml of the electrolyte solution and, under the inert atmosphere contained within the electrode chambers, electrolyzed at a maximum constant current of 300 μA for 6 days. The cathodic dissolution reaction resulted in the formation of a bright orange powder that formed mainly on and below the Ga_2Te_3 cathode, and a small number of orange needle-shaped crystals which grew both on the Ga_2Te_3 electrode and on the walls of the cathode chamber.

Reactions in this system have typically yielded less than 0.01 g of crystals (an average yield of 8% based on moles of Ga). The reactions are stopped when the insulating orange powder layer prevents further passage of current through the cell, and much of the Ga_2Te_3 electrode is left intact at the end of the experiment. The electrochemical yield (moles of crystalline product per moles of e- passed) is typically less than 1%, but as much as 12–15% if the powder is included. This powder, which may also be $[(C_6H_5)_4P]GaTe_2(en)_2$ (**7**), has not yet been completely characterized except for qualitative microprobe analyses which have yielded Ga:Te ratios of between 1:1.85 and 1:2.06.

X-ray structural analysis of the bright orange crystals of $[(C_6H_5)_4P]GaTe_2(en)_2$ (**7**) revealed the novel $GaTe_2(en)_2^{1-}$ anion which is shown in Fig. 8. The

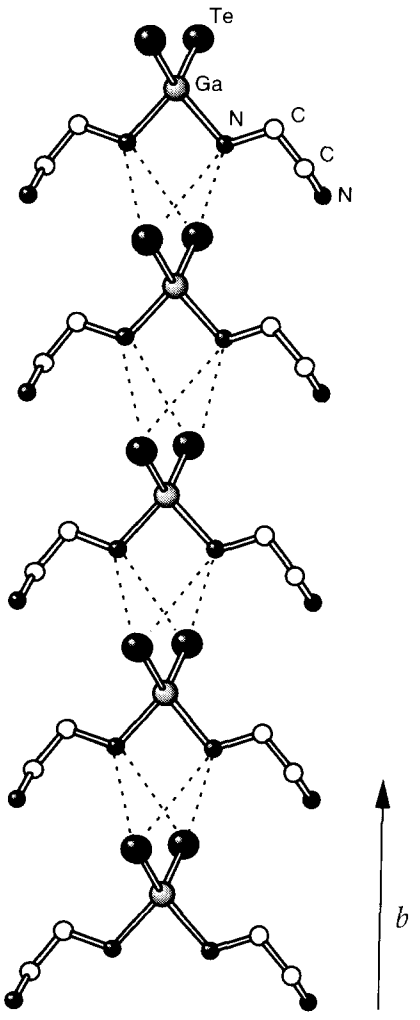

Fig. 8. The one-dimensional doubly hydrogen bonded chains in the structure of $[(C_6H_5)_4P]GaTe_2(en)_2$ (**7**). Some relevant bond distances and angles are as follows: Te–Ga, 2.509(1) Å; Ga–N, 2.081(7) Å; Te–Ga–Te, 125.7(1) Å; Te–Ga–N, 110.0(2) Å; Te–Ga–N′, 109.2(2) Å; N–Ga–N′, 85.2(4) Å. The Te–N non-bonded distances (represented by dotted lines) range from 3.750(7) to 3.793(7) Å, and the nearest N···N non-bonded distances are either 3.13(1) or 3.46(1) Å.

anion consists of Ga(III) in a distorted tetrahedral coordination environment. The gallium atom lies on the Wyckoff 4e special position in space group $C2/c$ on a twofold axis and is bonded to two crystallographically equivalent terminal tellurium atoms. The Ga–Te bond distance is 2.509(1) Å, which is 0.11 Å shorter than the sum of the Ga and Te covalent radii, 2.62 Å [96]. Owing to the paucity of structurally characterized Ga–Te compounds, it is difficult to make extensive comparisons with this Ga–Te bond distance. The four-membered Ga_2Te_2 ring in the compound $\{[(CH_3)_3CCH_2]_2GaTe(C_6H_5)\}_2$ has Ga–Te bond distances in the range 2.7435(8)–2.7623(8) Å [89], and $K_6Ga_2Te_6$ is composed of two edge-sharing $GaTe_4$ tetrahedra with Ga–Te bond distances of 2.591 Å (terminal) and 2.680 Å (bridging) [91]. In the solid state phases, the average Ga–Te bond distances in GaTe (monoclinic) [97a, b], GaTe (hexagonal) [98], Ga_2Te_3 [99] and Ga_2Te_5 [97] are 2.665, 2.61, 2.56, and 2.641 Å respectively. Therefore, it would appear that the $GaTe_2(en)_2^-$ anion has the shortest Ga–Te bond distance thus far recorded. This short Ga–Te bond distance can be rationalized if one considers the following resonance structures:

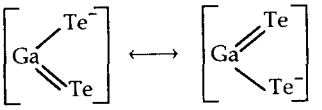

Such a description would lead one to believe that the Ga–Te bond distance of 2.509(1) Å is actually intermediate between a single and double bond and would help to explain this short distance relative to the other known Ga–Te bonds. However, it is impossible to confirm this speculation since no structures with a true Ga–Te double bond have yet been isolated.

The Te–Ga–Te bond angle of 125.7(1)° is greatly distorted from the ideal tetrahedral angle of 109.5°C by the repulsion of the large Te atoms which are 4.465 Å apart. The N–Ga–N angle is 85.2(4)°, bringing the inner ethylenediamine N atoms to within 2.816 Å of each other. The Te–Ga–N angles are 110.0(2)° and 109.2(2)°.

Unlike the corresponding sulfides and selenides, there are few examples of hydrogen bonding to telluride anions. Hydrogen bonding of an ethylenediamine molecule to Te_3^{2-} has been observed [100] with an N–Te distance of 3.46(6) Å, and CH_3OH has also been observed to hydrogen bond to the ends of a Te_4^{2-} anion [101] with the O–Te distance being 3.585(7) Å. The criteria for determining the evidence of a hydrogen bond in a crystalline solid was suggested by Hamilton and Ibers [102] as the observation of a distance between two non-hydrogen atoms, one of which is capable of donating electrons (tellurium in this case) and one of which is electronegative and bonded to hydrogen, which is less than the sum of the van der Waals radii. According to Pauling [96] this sum is 3.70 Å for Te–N, which is just 0.050 Å shorter than the closest Te–N contact of 3.750(7) Å and only 0.093 Å shorter than the longer N–Te contact of 3.793(7) Å. In $[(C_6H_5)_4P]GaTe_2(en)_2$ (**7**), however, we are dealing with two hydrogen bonds per tellurium atom and a formal Te^{2-} anionic radius instead of a Te atomic radius; both these reasons may contribute to the longer observed hydrogen bonding distances.

The individual chains of $GaTe_2(en)_2^-$ run parallel to the crystallographic b axis in sheets which are effectively isolated from one another by tetraphenylphosphonium cations. Individual chains within these rows have terminal ethylenediamine N–N contacts of

3.461 Å and are clearly not related by hydrogen bonding interactions. The Te–Te distance between rows of $GaTe_2(en)_2^-$ chains is 9.789 Å.

6.2. Synthesis and structure of $[(C_4H_9)_4N]_2In_2Te_4$

There are many compounds in the literature containing indium and the heavier chalcognides. Examples of one-dimensional materials are rarer but do indeed exist. The compound $Rb_4In_2S_5$, for instance, consists of edge-sharing InS_4 tetrahedra that form polymeric $In_2S_5^{4-}$ chains by corner sharing [103]. The compound $Rb_4In_2Se_5$ is isostructural to $Rb_4In_2S_5$ with the same one-dimensional chains [104]. In the compound $KInSe_2$, $InSe_4$ tetrahedra form adamantane-like In_4Se_{10} groups that are linked two-dimensionally via corners to form a layered material [104]. Polymeric one-dimensional indium tellurides include the compounds $XInTe_2$ (X = Na or K) [105], $Y_2In_2Te_4$ (Y = Ca or Ba) [106], $Na_5In_2Te_6$ [107] and $GaInTe_2$ [108]. Other solid state compounds in the indium telluride system include $LiInTe_2$ [109], InTeCl [110] and K_5InTe_4 [111].

There are many congruently melting telluride phases on the In–Te phase diagram [31]. These include In_2Te, InTe, In_2Te_3 and In_2Te_5. The In_2Te_5 phase was chosen for use as an electrode material since this phase is the most tellurium rich and should therefore be the most conductive.

Single crystals of $[(C_4H_9)_4N]_2In_2Te_4$ (**8**) were prepared by the cathodic dissolution of an In_2Te_5 alloy electrode which was made as previously described [112]. The electrochemical cell was filled with a solution of 0.40 M tetrabutylammonium iodide in ethylenediamine which served as both a source of cations for the crystallization process and the supporting electrolyte. The cathodic dissolution reaction, which ran at a constant current of 1 mA immediately gave rise to a deep-red stream of anions which surrounded the cathode and then sank to the bottom of the cathode chamber. After 1 day the solution in the cathode chamber was dark red in color and transparent yellow plate-like crystals had been deposited on the In_2Te_5 electrode and throughout the cathode chamber. The deposition of this yellow crystalline layer (the elemental microprobe analysis of which showed an In:Te ratio of 1:1.97) on the In_2Te_5 electrode reduced the current flow to 300 μA where it was held for another 4 days. The dark-red catholyte solution was then filtered under a He atmosphere leaving transparent yellow plate-like crystals which were isolated with an approximate 35% yield (electrochemical yield, 12%). Exactly how the cathodic dissolution of an In_2Te_5 electrode in a concentrated solution of tetrabutylammonium iodide yields the one-dimensional chain compound $[(C_4H_9)_4N]_2In_2Te_4$ (**8**) is unclear at this time but may occur according to the following equation:

$$In_2Te_5 + 2(C_4H_9)_4NI \xrightarrow{4e^-} [(C_4H_9)_4N]_2In_2Te_4 + Te_x^{2-} \quad (1)$$

where Te_x^{2-} may be present as excess polytellurides in the catholyte solution, left as unreacted tellurium metal in the cathode, or perhaps some combination of both.

The bright yellow crystals of $[(C_4H_9)_4N]_2In_2Te_4$ (**8**) were the only solid products obtained from the dissolution reaction and were not obtained from a control experiment of powdered In_2Te_5 and tetrabutylammonium iodide in ethylenediamine. The crystals are unstable with respect to oxygen and moisture, decomposing immediately into a gray–black solid on exposure to the atmosphere.

The structure of $[(C_4H_9)_4N]_2In_2Te_4$ (**8**) consists of $InTe_4$ tetrahedra which are linked together by sharing opposite edges to form one-dimensional $In_2Te_4^{2-}$ chains. The $In_4Te_{10}^{8-}$ structural repeat unit is shown in Fig. 9. The unit cell contains four separate $In_4Te_{10}^{8-}$ chain fragments per unit cell translation along *a*. The In–Te bond distances in the In_2Te_2 four-membered rings within these units are in the range 2.786(2)–2.814(2) Å. The transannular In–In distances in these rings are in the range 3.697(5)–3.732(5) Å, and those of the Te–Te are 4.140(1)–4.188(2) Å. A unit-cell view showing a more complete picture of these chains is given in Fig. 10. The $In_2Te_4^{2-}$ chains run parallel to the crystallographic *a* axis and are effectively isolated from one another by tetrabutylammonium cations. These chains are isotypic with those found in the SiS_2 and $KFeS_2$ type compounds [74,75] and are closely related to those found in the solid state compounds $XInTe_2$ (X = Na or K) [105] and YIn_2Te_4 (Y = Ca or Ba) [106], but it would seem as though the compound $[C_4H_9)_4N]_2In_2Te_4$ (**8**) represents the first example of a telluride compound with this structure type containing organic cations and completely isolated metal chains.

Comparison of the one-dimensional indium telluride

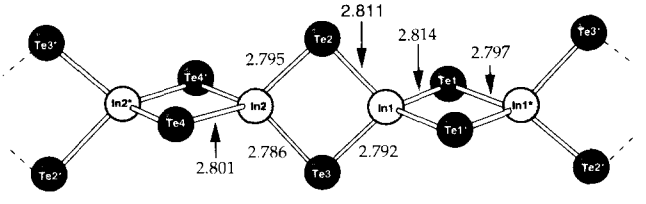

Fig. 9. The structure of the $In_2Te_4^{2-}$ chains in the one-dimensional indium telluride compound $[(C_4H_9)_4N]_2In_2Te_4$ (**8**) formed from the cathodic dissolution of an In_2Te_5 alloy electrode in a tetrapropylammonium iodide supporting electrolyte. The transannular nonbonded In–In and Te–Te distances range from 3.697(5) to 3.755(5) Å and 4.140(1) to 4.188(2) Å respectively.

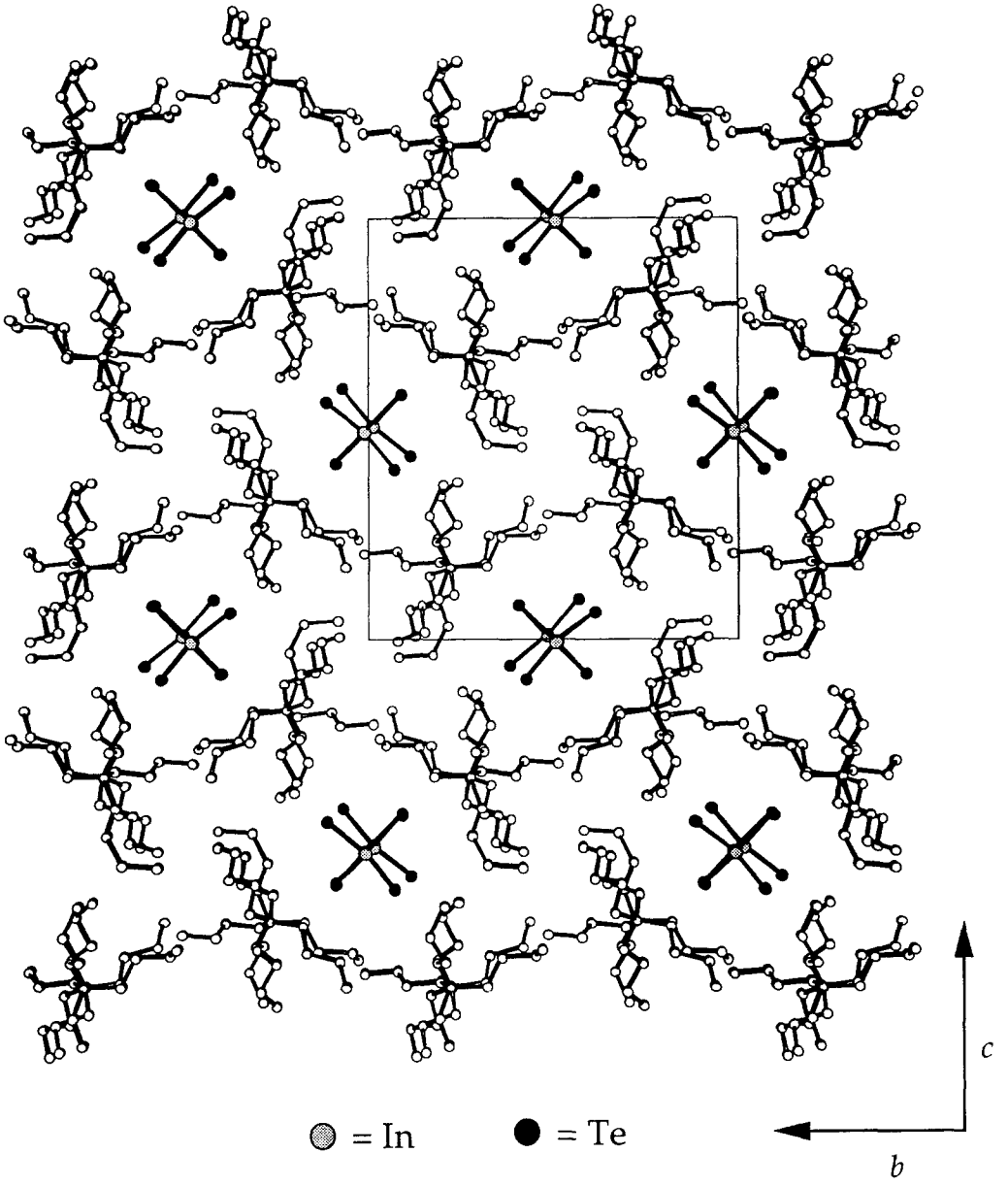

Fig. 10. Unit-cell view of the structure of $[(C_4H_9)_4N]_2In_2Te_4$ (**8**) down the crystallographic *a* axis showing the one-dimensional $In_2Te_4^{2-}$ chains which are completely isolated from each other in the solid state by tetrapropylammonium cations.

compound $[(C_4H_9)_4N]_2In_2Te_4$ (**8**) with other structurally characterized indium tellurides shows numerous structural similarities (based on the $InTe_4$ tetrahedral unit), and a general agreement in In–Te bond distance values. The structure of Na_5InTe_4, for example, consists of isolated $InTe_4$ tetrahedra with an average In–Te bond length of 2.788 Å [107]. A similar structure, $Na_5In_2Te_6$, also consists of $InTe_4$ tetrahedra, this time connected through common vertices to form "Zweiereinfach" chains which are further joined into ribbons through intermittent neighboring Te–Te bridges [107]. The average In–Te bond length in $Na_5In_2Te_6$ is 2.799 Å. Other compounds include the solid state materials $LiInTe_2$ [109], InTeCl [110] and K_5InTe_4 [111], the first of which crystallizes in the chalcopyrite structure type with In–Te bond distances of 2.768 Å. The compound InTeCl contains complex layers of strongly distorted $InTe_3Cl$ tetrahedra with In–Te bond distances varying from 2.752 to 2.883 Å. The structure of K_5InTe_4 has not been determined, the compound to date being characterized by X-ray powder diffraction and elemental analysis studies. All these compounds have been prepared by the high temperature fusion of stoichiometric amounts of the elements.

Structural similarities also exist between $[(C_4H_9)_4N]_2In_2Te_4$ (**8**) compound and indium sulfides and selenides. The compounds $Rb_6In_2S_6$ and

$Rb_4In_2S_5$, for instance, consist of edge-sharing InS_4 tetrahedra that form isolated $In_2S_6^{6-}$ anions in the former and polymeric $In_2S_5^{4-}$ chains by corner sharing in the latter [103]. One-dimensional chains (of $In_2Se_5^{4-}$) are also found in the isostructural $Rb_6In_2Se_6$ compound which was prepared by the high temperature fusion of stoichiometric mixtures of the elements [104]. Finally, in the compound $KInSe_2$, $InSe_4$ tetrahedra form adamantane-like In_4Se_{10} groups that are linked two-dimensionally via corners to form a layered material [104]. Other examples of compounds with very common InX_4 (X = S, Se, or Te) tetrahedral unit are likely to exist or will almost certainly be synthesized in the future. It should be noted here, however, that the cathodic dissolution method presented herein represents the first time that such a material was generated by an electrochemical process.

6.3. Synthesis and structure of $[(C_2H_5)_4N]_2As_2Te_5$

Prior to the synthesis of $[(C_2H_5)_4N]_2As_2Te_5$ (**9**), all the other structurally characterized arsenic telluride compounds were either anions (such as $As_4Te_6^{4-}$ or $As_{10}Te_3^{2-}$) or two- and three-dimensional solid state structures (such as As_2Te_3). The compound $[(C_2H_5)_4N]_2As_2Te_5$ (**9**) therefore represents the first example of a structurally characterized one-dimensional inorganic arsenic telluride polymer.

The electrochemical dissolution reaction that produces single crystals of $(C_2H_5)_4N]_2As_2Te_5$ (**9**) required the use of an As_2Te_3 alloy electrode which was prepared by the fusion of stoichiometric mixtures of the elements in a quartz container as previously described [113]. The easily melted silver–gray product was ground to a fine powder and recast into cylindrical electrodes which were incorporated into the electrochemical cell as previously described. All three chambers of the electrochemical cell were filled with approximately 10 ml of the electrolyte solution which consisted of 0.30 M tetraethylammonium iodide in ethylenediamine. The assembled electrochemical cell was attached to a constant-current power supply and electrolyzed at 300 μA for 5 days. The electrolyses resulted in the immediate formation of a dark-red stream of anions which completely surrounded the As_2Te_3 cathode and then slowly sank to the bottom of the cathode chamber. As more current was passed, the electrode dissolved and the catholyte became very dark as the polyanions increased in concentration. After 5 days, two crystalline products were isolated from the cathode chamber: thin red needles having an As:Te ratio of between 1:1.2 and 1:1.5 (based on multiple EDS analyses), and black spear-shaped crystals which appeared red in thin section having an As:Te ratio of 1:2.25–1:2.58. These crystals appear to be the only solid products obtained from the cathodic dissolution process, are isolated in an approximate 50:50 ratio and are not produced from a control experiment of powdered As_2Te_3 and tetraethylammonium iodide in ethylenediamine. The thin red needles have to date been unsuitable for single-crystal X-ray analysis and have only been incompletely characterized by EDS analysis. They are extremely air sensitive and very thin, making all attempts at their analysis extremely difficult. Variations in the electrolysis current (10–300 μA) and time of the electrolysis (1–5 days), as well as changes in the concentration of the supporting electrolyte (0.10–0.30 M) have been attempted to grow better samples of these crystals. All attempts, however, have resulted in the formation of the same extremely tiny needle-shaped and unsuitable crystals. Single-crystal X-ray analysis was, however, possible on the black spear-shaped crystals. This analysis revealed the new arsenic telluride one-dimensional polymer $[(C_2H_5)_4N]_2As_2Te_5$ (**9**). As in all previous experiments using nickel as the counterelectrode, a purple crystalline material, which had a Ni:I ratio of approximately 1:2, was deposited on and near the anode.

The arsenic and tellurium atoms in $[(C_2H_5)_4N]_2As_2Te_5$ (**9**) are present as novel one-dimensional $As_2Te_5^{2-}$ infinite chains which are separated in the solid state by $(C_2H_5)_4N^+$ cations. The structure of the $As_2Te_5^{2-}$ repeat unit is shown in Fig. 11. These chains run parallel to the crystallographic *c* axis and have the structure shown in the unit-cell diagram in Fig. 12. The polyanions that make up these chains can be considered in a formal sense to be built up from As–As-bonded As_2^{4+} dimers and planar Te_5^{6-} squares. The As–As bond length of the As_2^{4+} dimer, which lies astride the $\bar{1}$ site at $0, 0, \frac{1}{2}$, is 2.451(8) Å and can be compared with As–As distances of 2.517 Å in the α form of elemental arsenic [114] or the contacts in the range 2.357–2.498 Å as found in the As_7^{3-} [115] or As_{11}^{3-} [116] polyanions. The As_2^{4+} dimers are bonded to four neighboring Te atoms at 2.587(5) and 2.598(4) Å. These As–Te distances are similar to the As–Te distances of 2.604–2.614 Å for μ^2 bridging

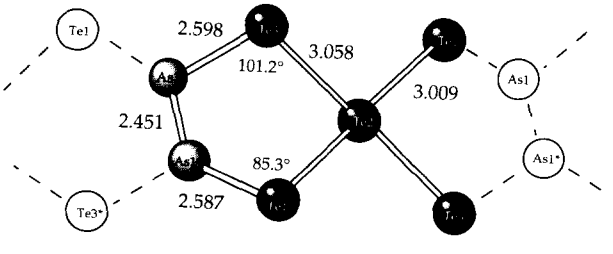

Fig. 11. The structure of the $As_2Te_5^{2-}$ chains in the one-dimensional arsenic telluride compound $[(C_2H_5)_4N]_2As_2Te_5$ (**9**) formed from the cathodic dissolution of an As_2Te_3 alloy electrode in a tetraethylammonium iodide supporting electrolyte.

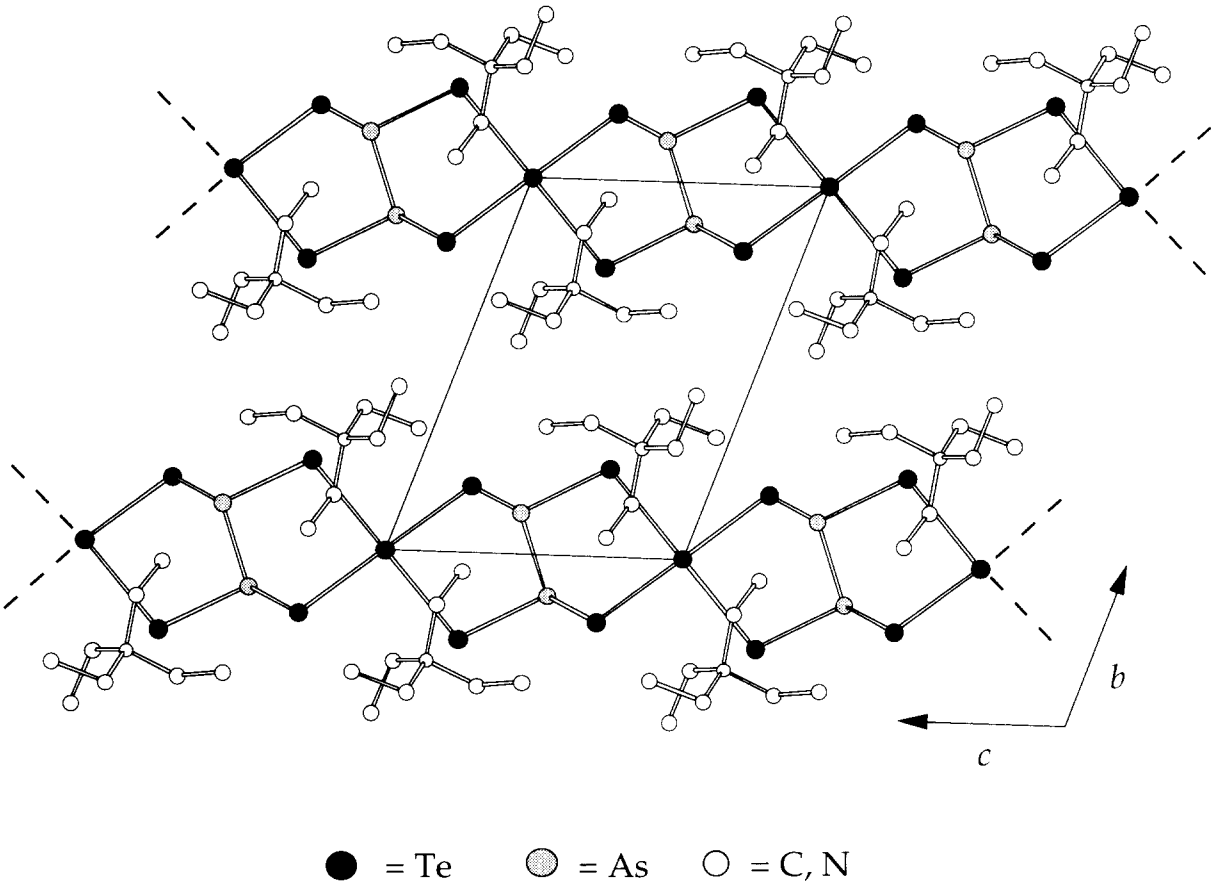

Fig. 12. Unit-cell view of the structure of $(Et_4N)_2[As_2Te_5]$ (**9**) showing the one-dimensional $As_2Te_5^{2-}$ chains running parallel to the crystallographic *c* axis. The chains are separated in the solid state by tetraethylammonium cations.

tellurium atoms in previously characterized arsenic tellurides [117].

The tellurium portion of the polyanion chain can be considered to be present as 36-electron $TeTe_4^{6-}$ units that are topologically similar to XeF_4 molecules [118]. Similar Te moieties can be recognized in Ga_2Te_5 [119]. However, the closest structural analogs to the one-dimensional chains in $[(C_2H_5)_4N]_2As_2Te_5$ (**9**), in terms of the $TeTe_4^{6-}$ units, are found in the one-dimensional $SnTe_5^{2-}$ chains present in K_2SnTe_5 [120a] and isotypic Rb_2SnTe_5 [120b], where the Sn^{4+} cations and As_2^{4+} dimers occupy similar positions within the chains with respect to the $TeTe_4^{6-}$ units. In all these materials containing $TeTe_4^{6-}$, the distance of the central tellurium to the remaining tellurium atoms falls in a surprisingly narrow range of around 3.05 Å. The distances per comparable repeat unit along the $SnTe_5^{2-}$ and $As_2Te_5^{2-}$ chains are very similar with values of 7.795 Å and 7.829 Å for $SnTe_5^{2-}$ and $As_2Te_5^{2-}$ respectively. The similarity of both charge and connectivity requirements of the Sn^{4+} cations and As_2^{4+} dimers suggest that it may be possible to prepare materials with a solid solution of different cations at the metal sites within the telluride chain as was recently found for the one-dimensional chains in $K_2HgSnTe_4$ [80]. In fact, the one-dimensional telluride chains in $K_2HgSnTe_4$ are related to the chains in $SnTe_5^{2-}$ by simply replacing the square planar Te with a tetrahedral Sn/Hg site which results in a halving of the *c* axis in $HgSnTe_4^{2-}$ (or $As_2Te_5^{2-}$) relative to $SnTe_5^{2-}$.

It is interesting to note that the compound $[(C_2H_5)_4N]_2As_2Te_5$ (**9**), like the other electrochemically synthesized arsenic telluride anion, $As_4Te_6^{4-}$ [10,57], contains direct As–As bonds. As noted earlier, neither the monoclinic nor the rhombohedral modifications of As_2Te_3, the starting electrode material, have any direct As–As interactions. These As–As interactions form the basis of a common building block that is found in both $As_2Te_5^{2-}$ and $As_4Te_6^{4-}$—an As_2Te_4 moiety. As shown in Fig. 13, which compares the structures of the two electrochemically synthesized arsenic tellurides, the $As_2Te_4^{4-}$ moiety (Fig. 13(A)) is found in both structures. This structural unit has not to date been prepared by an electrochemical method but has just recently been isolated through a high temperature fusion–extraction process [121]. In Fig. 13(B), one can see how two $As_2Te_4^{4-}$ units combine, with the loss of two tellerium atoms, to form the $As_4Te_6^{4-}$ Zintl

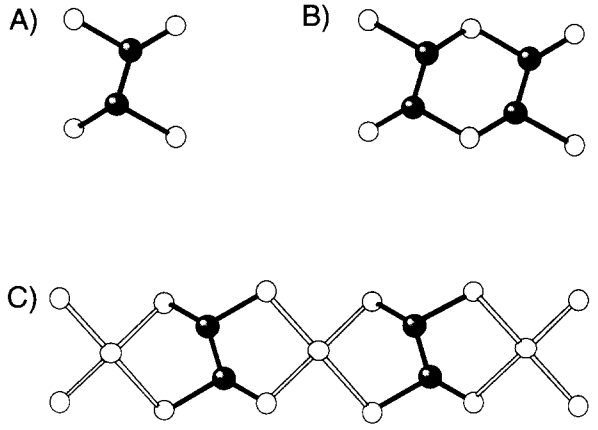

Fig. 13. (A) The $As_2Te_4^{4-}$ structural unit, (B) its incorporation into the arsenic telluride anion $As_4Te_6^{4-}$ and (C) one-dimensional chain material $As_2Te_5^{2-}$: ●, As.

anion. Fig. 13(C) shows how the $As_2Te_4^{4-}$ unit is incorporated in the $As_2Te_5^{2-}$ one-dimensional polymer, alternating between square planar Te_5^{6-} structural units.

6.4. Synthesis and structure of $[(CH_3)_4N]_4Hg_3Te_7 \cdot (0.5en)$

In the mercury telluride system, the first polyanion discovered was $[K\text{-}(2,2,2\text{-crypt})]_2HgTe_2 \cdot (en)$ [122], which was characterized during the pioneering studies of Corbett and coworkers on main group polyanions. The mercury telluride $[K\text{-}(2,2,2\text{-crypt})]_2HgTe_2 \cdot (en)$ was prepared by the extraction of an alkali metal alloy material of nominal composition KHgTe with 2,2,2-crypt in ethylenediamine. The extracts were reported to be yellow in color, indicating that the material extracted from this alloy contained no homoatomic Te–Te bonds (which are characteristically very darkly colored). The $HgTe_2^{2-}$ anion was found to be linear with two equivalent Hg–Te bond distances of 2.5890(8) Å.

Subsequently, Haushalter [123] reported the synthesis and structural characterization of two polynuclear mercury tellurides, namely the tetramer $[(C_4H_9)_4N]_4Hg_4Te_{12}$, and the one-dimensional polymer $[(C_6H_5)_4P]_2Hg_2Te_5$ [123]. It is interesting to note that both $Hg_4Te_{12}^{4-}$ and $Hg_2Te_5^{2-}$ were prepared by the extraction of exactly the same alloy, this time $K_2Hg_2Te_3$, with only the cation used to treat the extract being different. Another one-dimensional mercury telluride polymer, $[(C_2H_5)_4N]_2Hg_2Te_4$, has also just recently been synthesized from the extraction of this alloy in a tetraethylammonium iodide solution in ethylenediamine [124]. These observations suggest that at least three interconvertible species must be present in the ethylenediamine extracts of $K_2Hg_2Te_3$.

While several other mercury selenides and sulfides (which exist as both isolated anions and three-dimensional solids) are known [125], the only other mercury telluride anion reported in the literature is the $HgTe_7^{2-}$ anion [126].

The electrochemical dissolution reaction that produces the one-dimensional mercury telluride polymer $[(CH_3)_4N]_4Hg_3Te_7 \cdot (0.5en)$ (**10**) required the use of a Hg_2Te_3 alloy cathode [124]. Although the mercury–tellurium phase diagram does not contain an Hg_2Te_3 congruently melting phase (HgTe is the only one) [31], this particular composition was chosen because of our success with the ethylenediamine extractions of $K_2Hg_2Te_3$ alkali metal alloys, and because an alloy whose composition was tellurium rich was desired. This particular Hg_2Te_3 alloy was difficult to make because, on heating, the mercury tended to boil out of the melt rather than form the alloy. Once formed, however, the resulting regulus appeared homogeneous, was easily crushed into a fine powder and could be easily remelted to make electrodes. The final composition of these electrodes, however, was probably not strictly Hg_2Te_3 in all cases.

The cathodic dissolution reaction of the Hg_2Te_3 electrode took place in the electrochemical cell described above in a solution of approximately 0.15 M tetramethylammonium iodide in ethylenediamine. The electrolysis was begun at a maximum constant current of 100 μA and lasted for 10 days. Immediately on application of this current, intensely colored dark-red–purple streams of anions were produced, and they quickly surrounded the Hg_2Te_3 cathode, finally sinking to the bottom of the cathode chamber. Unlike most of the other cathodic dissolution reactions, however, this stream ceased to be produced after only a few hours, and a black crystalline layer was noticed growing on the Hg_2Te_3 cathode. The catholyte solution remained only light red–purple throughout the electrolysis, suggesting a rather low overall concentration of anions present. Throughout the electrolysis, crystals were found growing on the Hg_2Te_3 cathode, forming an insulating layer which eventually reduced the applicable current to less than 1 μA. The reaction was terminated after 10 days when crystals large enough for single-crystal X-ray analysis were seen. Most of these crystals were found growing on the Hg_2Te_3 cathode and the epoxy that surrounded it, but a few were noticed on the bottom and walls of the cathode chamber. The crystals were isolated in approximately 40% yield (electrochemical yield, 14%).

The novel one-dimensional mercury telluride compound $[(CH_3)_4N]_4Hg_3Te_7 \cdot (0.5en)$ (**10**) crystallizes in the space group $P\bar{1}$ (No. 2) with one complete $Hg_3Te_7^{4-}$ chain fragment, four tetramethylammonium cations and half an ethylenediamine molecule in the asymmetric unit. The structure of the $Hg_3Te_7^{4-}$ repeat unit is shown in Fig. 14. The complete structure of **10**

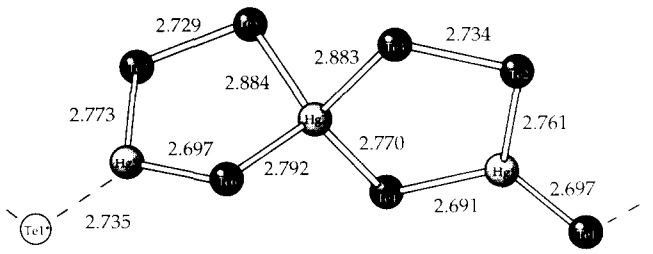

Fig. 14. The structure of the $Hg_3Te_7^{4-}$ repeat unit in the one-dimensional mercury telluride compound $[(CH_3)_4N]_4Hg_3Te_7 \cdot (0.5en)$ (**10**) formed from the cathodic dissolution of a Hg_2Te_3 alloy electrode in a tetramethylammonium iodide supporting electrolyte.

contains infinite one-dimensional $Hg_3Te_7^{4-}$ chains which are built up from $Hg_3Te_6^{2}$ moieties that are joined together into strands via single-atom tellurium (Te^{2-}) bridges. A section of the $Hg_3Te_7^{4-}$ chain is shown in Fig. 15(A). Here one can see how the $Hg_3Te_6^{2}$ moieties mentioned above are each made up of two fused Hg_2Te_3 five-membered rings which share a corner Hg atom (Hg(2)). Mercury atoms Hg(1) and Hg(3) in these units have approximately trigonal planar coordination with Te–Hg(1)–Te bond angles of 118°, 118° and 124°, and Te–Hg(3)–Te bond angles of 116°, 119° and 123°. The Hg(2) atom is in a tetrahedral environment with Te–Hg(2)–Te angles varying between 99° and 120° (average, 109.5°). While tetrahedral coordination is common for Hg^{2+}, this is only the second structurally characterized example in mercury tellurides ($Hg_4Te_{12}^{4}$ [123] contains the first). As expected, the $Te–Hg_{(tetrahedral)}$ bond distances are significantly longer than the $Te–Hg_{(trigonal)}$ bond distances. The four $Te–Hg_{(tetrahedral)}$ bond distances range from 2.770(2) to 2.884(2) Å with an average of

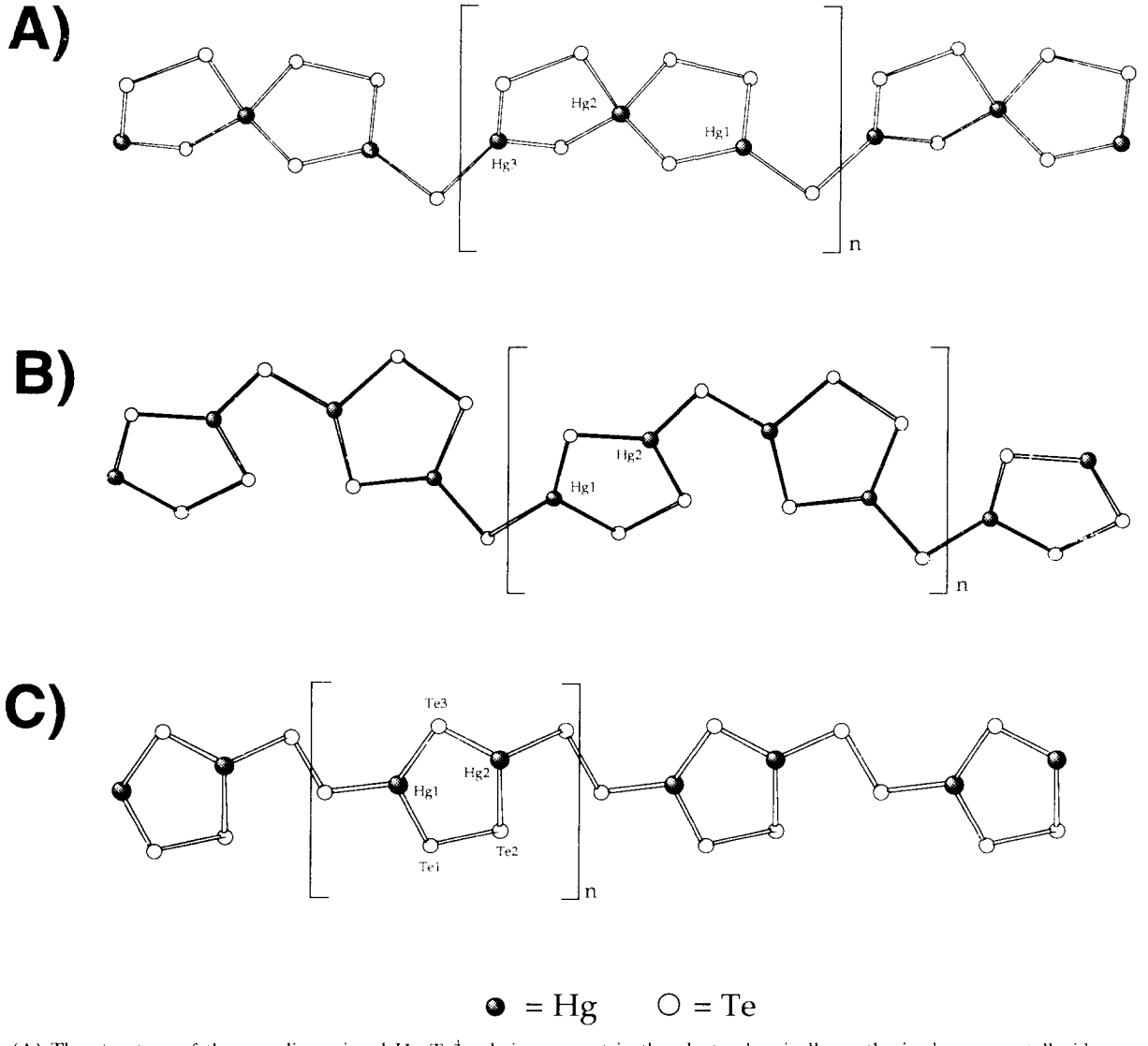

Fig. 15. (A) The structure of the one-dimensional $Hg_3Te_7^{4-}$ chains present in the electrochemically synthesized mercury telluride compound $[(CH_3)_4N]_4Hg_3Te_7 \cdot (0.5en)$ (**10**). The chains run parallel to the crystallographic *a* axis. (B) The structure of the one-dimensional $Hg_2Te_4^{2-}$ chains present in $[(C_2H_5)_4N]_2Hg_2Te_4$. (C) The structure of the one-dimensional $Hg_2Te_3^{2-}$ chains present in $[(C_6H_5)_4P]_2Hg_2Te_3$.

2.832 Å, while the six Te–$Hg_{(trigonal)}$ contacts range from 2.691(2) to 2.773(3) Å with an average of 2.726 Å. The Te–Te bond distances are 2.729(3) Å and 2.734(3) Å which are typical of many polytellurides.

Together with the four crystallographically independent $(CH_3)_4N^+$ cations in the structure, there is also an ethylenediamine molecule present in $[(CH_3)_4N]_4Hg_3Te_7 \cdot (0.5en)$ (**10**). The nearest Te–N intermolecular distance occurs between the Te(6) atom of the $Hg_3Te_7^{4-}$ chain and the N(5) atom of the ethylenediamine molecule and has a value of 3.88(3) Å. This distance is well outside the range of that expected for a Te–H–N hydrogen bond (Te–N distance should be 3.70 Å or less) [96], supporting the conclusion that the ethylenediamine molecule is merely present in the structure as a solvate of crystallization.

Although not isolated by the electrochemical method described herein, two other structurally related one-dimensional mercury telluride compounds exist. The first, $[(C_2H_5)_4N]_2Hg_2Te_4$, contains Hg_2Te_3 five-membered rings, which are not fused together but instead are connected by bridging tellurium atoms to form infinite one-dimensional chains [124]. The structure of a section of one of these infinite one-dimensional $Hg_2Te_4^{2-}$ chains is shown in Fig. 15(B), where some obvious structural similarities to the chains in $Hg_3Te_7^{4-}$ can easily be seen. In the structure of $[(C_2H_5)_4N]_2Hg_2Te_4$, both the Hg(1) and the Hg(2) atoms have approximately trigonal planar coordination, with Te–Hg(1)–Te angles of 116°, 119° and 124°, and Te–Hg(2)–Te angles of 109°, 116° and 135°. The Hg_2Te_3 five-membered rings that contain these mercury atoms are essentially planar, with distances of Hg(1) and Hg(2) from the least-squares planes of the three surrounding tellurium atoms being 0.05 Å and 0.18 Å respectively. The Hg_2Te_3 rings are joined together via monotelluride (Te^{2-}) bridges and have six crystallographically independent Hg–Te distances ranging from 2.683(4) to 2.791(5) Å (average distance, 2.728 Å). While the five-membered Hg_2Te_3 rings themselves are quite planar, the planes of these rings are tilted relative to one another such that the mercury telluride chain itself is somewhat buckled. The last example of a one-dimensional mercury telluride compound, $[(C_6H_5)_4P]_2Hg_2Te_5$, was actually isolated (chronologically) first [123]. In the structure of this compound (Fig. 15(C)), Hg_2Te_3 five-membered rings again form the basis of the one-dimensional strands which are this time connected together via ditelluride (Te_2^{2-}) bridges. Each Hg_2Te_3 five-membered ring in $[(C_6H_5)_4P]_2Hg_2Te_5$ contains two crystallographically independent mercury atoms, Hg(1) and Hg(2), which are present in approximately trigonal planar environments. The Hg(1) atom is about 0.1 Å out of the Te(1)–Te(2)–Te(3) plane, and that of the Hg(2) atom is 0.5 Å out of this plane. The average of the six Hg–Te bond distances is 2.714 Å, which can be compared with the average mercury to two-coordinated tellurium contacts in $Hg_4Te_{12}^{4-}$ (2.737 Å), or the other two one-dimensional mercury telluride compounds discussed above. Unlike the twisted structures of the $Hg_3Te_7^{4-}$ and $Hg_2Te_4^{2-}$ one-dimensional chains, the entire $Hg_2Te_5^{2-}$ chain is essentially planar.

Interestingly, none of Haushalter's mercury telluride compounds were isolated from the cathodic dissolution reactions using the Hg_2Te_3 alloy electrodes in $(C_4H_9)_4NI$, $(C_6H_5)_4PBr$ or $(C_2H_5)_4NI$ supporting electrolytes [10]. This phenomenon has been observed for several of the cathodic dissolution experiments discussed thus far, which typically yield different products from their extraction counterparts.

Although rare, other examples of species containing trigonal planar coordinated Hg atoms are known, such as $Hg_3O_3Cl_2$ [127] and $[(CH_3)_3S]HgI_3$ [128]. The above examples show how this coordination is favored in mercury tellurides, as it is found in both the $Hg_4Te_{12}^{4-}$ and $HgTe_7^{2-}$ anions, as well as in all three of the one-dimensional mercury telluride chains.

7. Electrochemical synthesis of extended structures

Inorganic molecular sieves such as zeolites have been extensively used by the petrochemical and refining industries as catalysts and in separation processes (for a review of zeolites and their properties see [129]). These zeolites are typically aluminosilicates whose framework structures are formally constructed from $(SiO_4)^{4-}$ and $(AlO_4)^{5-}$ tetrahedra that share vertices. These tetrahedra can connect in a variety of ways to form pores that vary in shape, size and dimensionality. The aperture dimensions of these pores control the accessibility of the zeolite's internal volume in such a way that molecules that are too large will be completely excluded or "sieved' out whereas those of suitable dimensions can enter into the large internal volume of the zeolite where they can undergo ion exchange or catalysis reactions with the zeolite's highly active surface sites. Most of the traditional and advanced applications for zeolites are based on this ability of these open crystalline structures to incorporate and exchange selectively both charged and neutral species within the void spaces and interconnecting channels within the zeolite, while at the same time having all outcomes of the reactions governed by shape-selective constraints.

Almost all crystalline molecular sieves and microporous materials to date have been based on oxide frameworks. This is not surprising as such frameworks are typically stable into the 400–600 °C temperature range necessary to remove the organic template and

free the intercrystalline void volume for adsorption or catalysis. If one were able to design a non-oxide-based microporous framework material, it would have the disadvantage of being less thermally stable, but have the added potential for interesting electronic properties not possible in the corresponding insulating microporous oxide materials.

Bedard et al. [130] have made the first crystalline microporous metal sulfides. These novel materials were based on germanium(IV) and tin(IV) sulfide frameworks and were synthesized hydrothermally in the presence of alkylammonium templating agents. They have shown that at least eight different alkylammonium and amine species can direct the structures of these microporous sulfides, giving rise to 12 novel structure types which possess no analogs in microporous oxide chemistry. Because of the greater propensity of sulfides to form fused three-ring building units, these microporous metal-sulfide-based solids typically show substantially more pore volume than most of the microporous oxides. In their experiments, Bedard et al. have also shown that at least ten different main group and transition metal elements can be incorporated into these sulfide frameworks which should lead to potentially interesting catalytic behavior.

More recently, Dhingra and Kanatzidis [131] and Parise [132] have constructed extended chalcogenide-containing solids based on polyselenide and antimony sulfide building blocks. These polychalcogenide two- and three-dimensional compounds are rare and represent a new class of materials which have not only the ability to incorporate and exchange ions but also the possibility of new and interesting electrical and optical properties. One of the compounds, constructed by Dhingra and Kanatzidis, $[(C_6H_5)_4P]In(Se_6)_2$, for example, is a semiconductor ($k \leq 10^{-6}$ S cm^{-1}) with an estimated band gap of 1.42 eV. It is thermally stable to a temperature of 350 °C and has been shown to be capable of ion exchange reactions with other R_4N^+ or R_4P^+ (R = alkyl or aryl group) cations of similar size and shape. In Parise's open framework $[(CH_3)_4N]Sb_3S_5$ compound, fused sheets of edge-linked Sb_2S_2 units that are further cross-linked in two directions form a system of interconnecting channels in which $(CH_3)_4N^+$ molecules reside. This compound's optical, electronic and sorption properties are currently under investigation. Both of these new types of extended two- and three-dimensional non-oxide materials have been prepared by hydrothermal techniques at temperatures of between 180 and 200 °C. These hydrothermal techniques have been used extensively in the synthesis of microporous oxides and now appear to be the primary source of synthesis for these types of material. While much interest and extensive work are currently being conducted in this area, it is interesting to note that no extended telluride network or microporous telluride materials like these have yet been synthesized.

Although a few 15-membered clusters and one-dimensional chain materials have been synthesized via the cathodic dissolution of telluride electrodes, the synthetic method presented herein seems to favor the production of highly charged small molecules, without multiple Te–Te bonds, which are completely surrounded by organic cations. The exact opposite is needed if a three-dimensional telluride network is to be formed, namely a nearly neutral structure with multiple Te–Te bonds that is capable of surrounding organic cations. Attempts have been made to vary the experimental conditions to produce larger extended structures using small tetraalkylammonium cations $[(CH_3)_4N^+]$, inorganic cations (Na^+, K^+ and Rb^+) and even inorganic dications (Mg^{2+} and Ca^{2+}), all of which have resulted in either the isolation of molecular anions or, in the case of the inorganics, no crystals at all.

In order for the electrochemical synthesis of a three-dimensional telluride network to be feasible, a way of producing an excess of tellurium in the form of extended polytelluride chains is necessary. Extended chains of polychalcogenides from two to six members are known, and have been synthesized by the standard high temperature and extraction techniques [2]. Several polytelluride compounds with these structures have also been isolated by the cathodic dissolution of telluride alloy electrodes [10]. However, for the electrochemical synthesis to work, some combination of the generation of a less charged anionic species combined with these extended telluride chains is necessary. One possible way for this to be accomplished would be to make the starting alloy tellurium rich. Presumably such an electrode would contain the congruently melting phase and excess tellurium. Upon dissolution, fragments of the antimony telluride phase and polytelluride chains should dissolve from the electrode and could subsequently combine in solution to form an extended three-dimensional structure by "wrapping" around the organic cations present in the supporting electrolyte.

7.1. Synthesis and Structure of $[(C_2H_5)_4N]_2Te_{12}$

Shiny silver needle-like crystals of $[(C_2H_5)_4N]_2Te_{12}$ (**11**) were prepared by the cathodic dissolution of an $SbTe_{10}$ alloy electrode in a 0.30 M solution of tetraethylammonium iodide in ethylenediamine in an electrochemical cell as described previously [133]. The $SbTe_{10}$ phase does not exist on the Sb–Te phase diagram [31], but this stoichiometry was chosen as an electrode material because it presumably contained the congruently melting Sb_2Te_3 phase and excess tellurium. It was hoped that electrolysis of this elec-

trode material would give rise to both antimony telluride and polytelluride species which could combine in solution to form an extended structure. Although the product $[(C_2H_5)_4N]_2Te_{12}$ (**11**) was shown to contain no antimony, the stoichiometry of the cathode is necessary as the electrolysis of pure tellurium electrodes produced only simple polytellurides [10].

The cathodic dissolution reaction, which was run at a constant current of 300 μA, immediately gave rise to a deep-red–brown stream of polyanions which surrounded the $SbTe_{10}$ cathode and then sank to the bottom of the cathode chamber. After electrolysis for only 1 day, the catholyte solution was so intensely colored that the $SbTe_{10}$ cathode was no longer visible. In two out of five cells that produced them, crystals did not appear in the cathode chamber until after electrolysis for about 10 days, and these were observed primarily growing from the $SbTe_{10}$ cathode and from the surface of the sintered glass frit facing the cathode. The electrolysis was allowed to progress for another 5 days (15 days total) after which time the contents were isolated. At the end of the electrolysis, nearly all the $SbTe_{10}$ cathode either had disintegrated into a silver–gray powder (which was found on the bottom of the cathode chamber) or had been transformed into crystals (also present on the bottom of the cathode chamber as well as growing from the inner surface of the cathode frit). Some of the crystals were greater than 5 mm in length. The color of the catholyte solution was an intense dark brown, suggesting that a significant concentration of antimony-containing polyanions were present in it. The chemical yield for $[(C_2H_5)_4N]_2Te_{12}$ was 54% (electrochemical yield, 18%). EDS analysis of several single-crystal-looking shards resulted in the observation of traces of antimony, consistent with the stoichiometry of the electrode material. Samples sent to the Schwarzkopf Microanalytical Laboratories (Woodside, NY) for elemental analysis also showed traces of antimony, but far less than expected if pure electrode material were analyzed. Found: Sb, 4.99, Te, 75.29. $SbTe_{10}$ calc.: Sb, 8.71; Te, 91.29%.

The extremely unusual structure of $[(C_2H_5)_4N]_2Te_{12}$ (**11**) consists of puckered Te_{12}^{2-} anions weakly bonded into a pseudo-two-dimensional sheet which is interleaved with Et_4N^+ cations giving alternating organic and inorganic layers within the solid. The Te_{12}^{2-} structural repeat unit is shown in Fig. 16, and a section of the pseudo-two-dimensional polytelluride layer it forms is shown in Fig. 17. Such polytelluride layered materials are rare, the closest analog being the alkali metal telluride compound, $RbTe_6$, recently isolated by Sheldrick and Schaff [134]. This compound contains Te_6 rings (which resemble cyclohexane in the chair conformation) that are connected into sheets via Te–

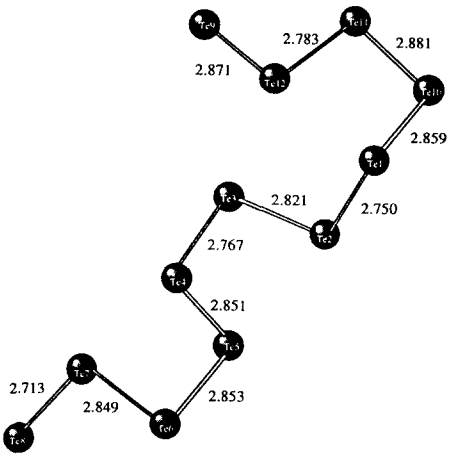

Fig. 16. The structure of the Te_{12}^{2-} repeat unit in the pseudo-two-dimensional layered compound $[(C_2H_5)_4N]Te_{12}$ (**11**). The compound was formed from the cathodic dissolution of an $SbTe_{10}$ alloy electrode in a tetraethylammonium iodide supporting electrolyte.

Te bonds involving four out of the six Te atoms in each ring. Individual sheets of the anionic tellurium network, containing both shorter (near 2.8 Å) and longer (near 3.2 Å) Te–Te interactions, are separated in the solid state by ribidium cations. In $[(C_2H_5)_4N]_2Te_{12}$ (**11**), the individual Te_{12}^{2-} anionic layers are separated in the crystallographic *b* direction by tetraethylammonium cations as shown in Fig. 18.

The twisted Te_{12}^{2-} polytelluride chain found in $[(C_2H_5)_4N]_2Te_{12}$ (**11**) represents the longest polychalcogenide chain isolated thus far, but this is only one of the unusual features present in the structure. The structure of the tellurium layers in $[(C_2H_5)_4N]_2Te_{12}$ (**11**) can be compared with the aforementioned $RbTe_6$ but an even more closely related structure is that of elemental tellurium, which has only one crystalline form [135] that is composed of a network of helical chains. Elemental Te crystallizes in the enantiomorphic space group $P3_121$ and consists of infinite helical chains running parallel to [001]. Within the infinite spiral there is only a single unique Te–Te distance of 2.835(2) Å, but each Te atom in the spirals contacts four additional Te atoms on adjacent chains (at distances of 3.495(3) Å) to give it a distorted six-coordinated environment. This 3.5 Å contact is far less than the van der Waals radius of 4.40 Å and represents a bonding interaction. All Te–Te–Te angles within the chain are 103.2(1)°. The Te portion of $[(C_2H_5)_4N]_2Te_{12}$ (**11**) likewise consists of a mixture of short, long and non-bonded Te–Te interactions, but these distances fall into three well-defined separate groups. The normal Te–Te covalent single bonds in the range 2.713–2.881 Å are all found within the Te_{12}^{2-} moiety. As illustrated in Fig. 17, these Te_{12}^{2-} chains are bonded together into an infinite, relatively planar two-

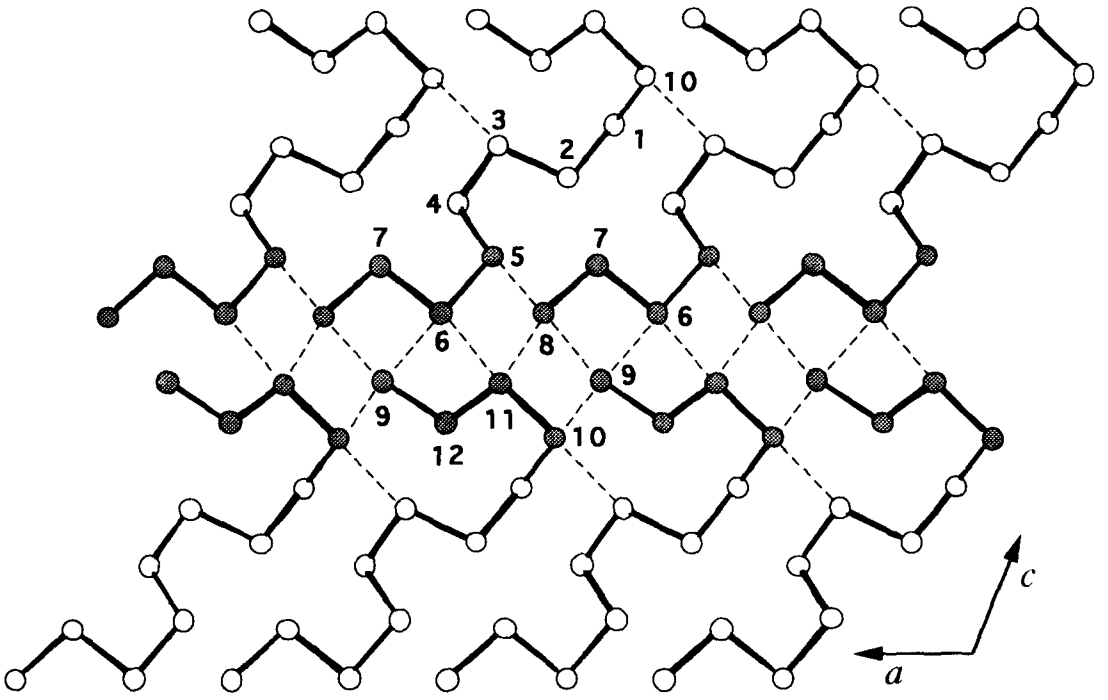

Fig. 17. A view nearly perpendicular to the infinite two-dimensional sheet of Te_{12}^{2-} anions in $[(C_2H_5)_4N]_2Te_{12}$ (**11**). The Te–Te covalent single bonds are represented by dark lines and the weaker bonding interactions in the 2.88 Å $< d_{Te\text{-}Te} <$ 3.50 Å are drawn as broken lines.

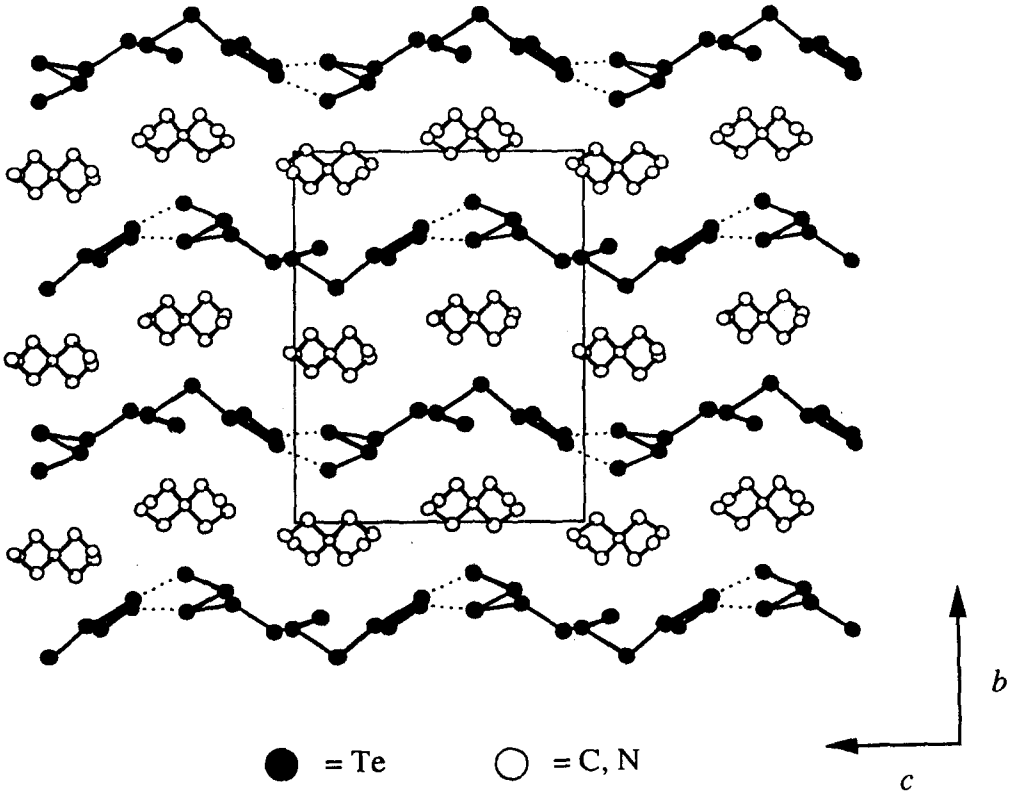

Fig. 18. Unit-cell view of the structure of $[(C_2H_5)_4N]_2Te_{12}$ (**11**) down the crystallographic *a* axis. Here one can see that individual ribbons of Te_{12}^{2-} are only loosely held together into sheets via Te–Te through-space interactions (represented as dotted lines).

dimensional net. The Te–Te interactions connecting the Te_{12}^{2-} chains into the layer are in the range 3.162–3.504 Å nearly all of which are significantly shorter than the intrachain 3.495(3) Å contacts in elemental Te mentioned above. As can be seen in Fig. 17, the intermediate length Te–Te contacts are distributed almost exclusively among the ends of adjacent Te_{12}^{2-} chains with the central atoms of each chain possessing either short covalent Te–Te single bonds or long van der Waals contacts. The remaining interactions are non-bonding and lie at distances greater than 3.764 Å. The pseudo-two-dimensional layers of Te_{12}^{2-} chains in $[(C_2H_5)_4N]_2Te_{12}$ (**11**) are separated in the crystallographic *b* direction by tetraethylammonium cations as shown in Fig. 18, resulting in a material containing alternating organic and inorganic layers.

8. General discussion

An interesting and yet unexplained observation of the electrochemical synthetic method described herein is that the stoichiometries of the anions isolated (as $A_xB_y^{n-}$) are typically different from the congruently melting telluride phase (AB) used to make the electrode itself. The structures of these anions also bear no resemblance to the structures of the electrode materials (which have in most cases been characterized by X-ray powder diffraction studies and consist of extended three-dimensional networks or layered materials). In a given system, when the supporting electrolyte is changed, the anions isolated are also typically different in both charge and stoichiometry from each other (even though they were generated from the same starting electrode material). Whether all this is a result of the dissolution process, a complex equilibrium situation that exists between all the anions generated, or some kind of chemical reaction that is influenced by the particular cation present, is not known at this time. Whatever the reason for this behavior, the technique has allowed us to isolate very different anions from the same starting electrode materials simply by changing the composition of the supporting electrolyte.

In no case was the polyanion generated by the electrochemical dissolution process able to be produced by simply grinding the alloy and adding it to an ethylenediamine solution containing the tetraalkylammoniun cation. Hence, one can see the importance of the application of current to the cathode, which causes the cathode to dissolve into the highly charged anionic species. The rate at which the cathode dissolved, which was adjustable by the amount of current applied to the cathode, did not seem to have any effect on the products isolated. Therefore reactions were typically run at the maximum current allowed. An interesting and unfortunately unexplored area of our research was the effect of potential on the cathodic dissolution process. This aspect remains an area of interest and will be addressed at a later date.

While almost all the heavier main group telluride electrodes have resulted in the formation of deeply colored streams of anionic species, not all have resulted in the isolation of crystalline compounds. Typically, for a given telluride alloy electrode material, all the organic tetraalkylammonium halide supporting electrolytes mentioned in the preceding sections were tried [10]. Purely inorganic supporting electrolytes, such as RbI or KI, yielded no single-crystal products in any system. In all cases except for the antimony telluride system, only one or perhaps two new crystalline products were obtained. Thus, for example, in the indium telluride system (In_2Te_5 electrode), only tetrabutylammonium (TBA^+) and tetrapropylammonium (TPA^+) cations worked, yielding single crystals containing the same isostructural one-dimensional $In_2Te_4^{2-}$ chains. No single-crystal materials were isolated from this system when either tetraethylammonium (TEA^+) or tetramethylammonium (TMA^+) cations were used and, using tetraphenylphosphonium (TPP^+) cations, crystals of polytellurides were the only solid products. Similar results were obtained in the arsenic telluride system (As_2Te_3 electrode), where only TMA^+ and TEA^+ cations yielded crystalline products and, in the gallium telluride system (Ga_2Te_3 electrode), where only TPP^+ worked (all others yielding no crystalline products). The antimony telluride system (Sb_2Te_3 electrode) was indeed an exception, for it seemed that every tetraalkylammonium cation used as a supporting electrolyte worked (including TPP^+ and TBA^+ which yielded crystals that have unfortunately been unsuitable for single-crystal X-ray analysis thus far) and, in several cases, even gave two different crystalline products from the same supporting electrolyte!

Of the heavier main group telluride electrodes that were tried, Pb_2Te_3 and Bi_2Te_3 gave no single-crystal lead telluride or bismuth telluride products (although the Pb_2Te_3 gave polytelluride crystals in a TEA^+ supporting electrolyte). This was a very disappointing result, as virtually any single-crystal products obtained from either of these systems would have been new. The problems associated with these systems may have been the result of impurities in the solvent (ethylenediamine) or supporting electrolytes, for many of the reactions tried resulted in the decomposition of the electrode material (as evidenced by powders obtained upon isolation of the catholyte contents). These systems are expected to be more sensitive to impurities in the solvent and are also expected to be more unstable

than their lighter main group analogs by virtue of weaker M–Te bonds; both these reasons may have prevented the isolation of crystalline products.

With the exception of the two gold telluride Zintl anions isolated, the transition metal telluride electrodes essentially yielded no crystalline products. Electrode materials of $AgTe_2$, $CuTe_2$, $FeTe_2$ and $PdTe_2$ were tried in various supporting electrolytes. In the $PdTe_2$ system, no streams of anions were even noticed. In the $FeTe_2$ system, deep-purple streams of anions were observed in several electrolytes, but no crystals were ever obtained. The copper and silver telluride electrodes yielded polytelluride crystals in a TPP^+ supporting electrolyte, but no crystalline materials in any other. Other than these, the transition metal tellurides were not explored in great detail.

From these results it can be seen not only that it is impossible to predict which cations will work with which electrode system but also that one has no idea what the products will be even when a particular cation does work. We are still unable to direct the synthesis of Zintl compounds or chalcogenide-containing materials using this electrochemical technique–a problem that is shared with the other high temperature fusion and extraction routines. Clearly more work needs to be done with these systems before we can ever succeed in predicting the outcomes of these reactions.

9. Future directions

As this technique is still in its infancy, there are many possible future directions that it might take on, many of which are currently under investigation in our laboratory. One could imagine, for instance, the extension of the synthetic technique to mixed metal selenides, arsenides and/or antimonides, as there is no particular reason why it must be used exclusively for the synthesis of tellurides. This aspect would have the advantage of extending the synthetic technique to an even wider range of materials using alloy electrodes made from the congruently melting phases in the Se, As and Sb systems. Zintl anions containing these elements exist and are currently being prepared by the standard high temperature and extraction routes mentioned before. Here, however, one has to be even more careful with respect to the purification of the solvent and supporting electrolytes as these systems are much more reactive than the corresponding tellurides. Still, since the cathodic dissolution of telluride electrodes gave rise to the isolation of so many new compounds, it would be interesting to see what new Zintl anions could be prepared from the cathodic dissolution of these non-telluride materials.

One could also imagine the use of ternary or quarternary electrode materials for the potential synthesis of multielement Zintl anions. If the cathodic dissolution of ternary electrode materials leads to the isolation of ternary Zintl anions, then a convenient and facile synthesis of these species, of which there are very few reported in the literature, would become a reality. Although not studied in great detail, several attempts to make these ternary Zintl anions from extractions of quaternary alloys have resulted in the isolation of only binary Zintl anion products. Examples include the extracts of KAuAsTe and KAuGeTe which both yield the binary Zintl anion $Au_2Te_4^{2-}$ [2h] and those of $KCuAsTe_3$ which yield the previously characterized arsenic telluride dianion $As_2Te_6^{2-}$ [56]. It has been shown that binary alloy electrodes dissolve to yield binary Zintl anions and, while having an alloy electrode containing three metals does not guarantee that they will all dissolve and form a ternary product, at least this possibility exists and is currently being explored.

Some other areas of potential exploration include the use of mixed organic–inorganic supporting electrolytes and variations in the solvent. The advantage of using a mixed organic–inorganic supporting electrolyte would be to vary the size and shape of cations present in the supporting electrolyte. This should, in theory, help in the crystal packing and, in turn, result in the isolation of more crystalline products. The more variations in terms of differently shaped cations around, the more likely one would be to isolate a crystalline product. Such systems containing a mixture of organic and inorganic templates have worked well in the hydrothermal synthesis of molybdenum phosphates [136], many of which would not crystallize without such a mixture. Although to date no crystalline compounds have been isolated using purely inorganic supporting electrolytes, the compound $Rb_2[(C_2H_5)_4N]_2Sn_2Te_6$ has been prepared in a mixed supporting electrolyte containing RbI and $(C_2H_5)_4NI$ [10]. The isolation of this compound provides evidence that inorganic cations can be useful in the crystallization process and could perhaps help in the systems where no solid products have yet been isolated.

As for the effect of the solvent, Zintl anions have been prepared in liquid NH_3, tetrahydrofuran and DMF, and it would be interesting to see what effect, if any, these solvents might have on the electrochemical synthesis (which has been done thus far exclusively in ethylenediamine). Furthermore, changing solvents would have the added advantages of introducing new cations which are insoluble in ethylenediamine, or improving the yields of compounds already produced by increasing the solubility of supporting electrolytes barely soluble in en. Since it has been shown that

varying the cations in the supporting electrolyte has a drastic effect on the products isolated, such manipulations should result in the isolation of new Zintl compounds.

Acknowledgments

The authors wish to thank Dr. Douglas M. Ho and Dr. Sandeep S. Dhingra for their work on the crystal structures of several of the compounds mentioned in this manuscript and Mr. Michael J. Souza for the construction of the electrochemical cells used in our experiments.

References

[1] (a) R. Nesper, *Angew. Chem., Int. Ed. Engl., 30* (1991) 789; (b) R. Nesper, *Prog. Solid State Chem., 20* (1990) 1; (c) H.G. von Schnering and W. Hönle, *Chem. Rev., 88* (1988) 243; (d) P. Böttcher, *Angew. Chem., Int. Ed. Engl., 27* (1988) 759; (e) H. Schäfer, *J. Solid State Chem., 57* (1985) 97; (f) H. Schäfer, *Annu. Rev. Mater. Sci., 15* (1985) 1; (g) H. Schäfer and B. Eisenmann, *Rev. Inorg. Chem., 3* (1981) 29; (h) H.G. von Schnering, *Angew. Chem., Int. Edn. Engl., 20* (1981) 33; (i) H. Schäfer, B. Eisenmann and W. Müller, *Angew. Chem. Int. Edn. Engl., 12* (1973) 694, and references cited therein.

[2] R.C. Haushalter, B.W. Eichhorn, A.L. Rheingold and S.J. Geib, *J. Chem. Soc., Chem. Commun.*, (1988) 1027; (b) R.C. Haushalter, *J. Chem. Soc., Chem. Commun.*, (1987) 196; (c) C. Belin and H. Mercier, *J. Chem. Soc., Chem. Commun.*, (1987) 190; (d) R.C. Burns and J.D. Corbett, *Inorg. Chem., 24* (1985) 1489; (e) R.C. Haushalter, B.W. Eichhorn, A.L. Rheingold and S.J. Geib, *J. Chem. Soc., Chem. Commun.*, (1985) 1207; (f) J.D. Corbett, *Chem. Rev., 85* (1985) 383; (g) S.C. Critchlow and J.D. Corbett, *Inorg. Chem., 24* (1985) 979; (h) R.C. Haushalter, *Angew. Chem. Int. Edn. Engl., 24* (1985) 432, 433; (i) R.C. Haushalter, *Inorg. Chim. Acta, 102* (1985) L37; (j) J.C. Huffman, J.P. Haushalter, A.M. Umarji, G.K. Shenoy and R.C. Haushalter, *Inorg. Chem., 23* (1984) 2312; (k) R.G. Teller, L.J. Krause and R.C. Haushalter, *Inorg. Chem., 22* (1983) 1809; (l) J.D. Corbett, S.C. Critchlow and R.C. Burns, in A. Cowley (ed.), *Rings, Clusters and Polymers of the Main Group Elements, ACS Symp. Ser., 232* (1983) 95–110; (m) S.C. Critchlow and J.D. Corbett, *Inorg. Chem., 21* (1982) 3286; (n) R.C. Burns and J.D. Corbett, *J. Am. Chem. Soc., 104* (1982) 2804; (o) R.C. Burns and J.D. Corbett, *J. Am. Chem. Soc., 103* (1981) 2627; (p) J.D. Corbett and P.A. Edwards, *J. Am. Chem. Soc., 99* (1977) 3313; (q) C.H.E. Belin, J.D. Corbett and A. Cisar, *J. Am. Chem. Soc., 99* (1977) 7163; (r) P.A. Edwards and J.D. Corbett, *Inorg. Chem., 16* (1977) 903; (s) L. Diehl, K. Khodadadeh, D. Kummer and J. Strähle, *Z. Naturforsch. 31b* (1976) 522; (t) L. Diehl, K. Khodadadeh, D. Kummer and J. Strähle, *Chem. Ber., 109* (1976) 3404; (u) D.G. Adolphson, J.D. Corbett and D.J. Merryman, *J. Am. Chem. Soc., 98* (1976) 7234; (v) J.D. Corbett and P.A. Edwards, *J. Chem. Soc., Chem. Commun.*, (1975) 984; (w) J.D. Corbett, D.G. Adolphson, D.J. Merryman, P.A. Edwards and F.J. Armatis, *J. Am. Chem. Soc., 97* (1975) 6267; (x) D. Kummer and L. Diehl, *Angew. Chem. Int. Ed. Engl., 9* (1970) 895, and references cited therein.

[3] (a) B. Dietrich, J.M. Lehn and J.P. Sauvage, *J. Am. Chem. Soc., 92* (1970) 2916; (b) B. Dietrich, J.M. Lehn and J.P. Sauvage, *Tetrahedron Lett.*, (1969) 2885, 2889.

[4] M.T. Lok, F.J. Tehan and J.L. Dye, *J. Phys. Chem., 76* (1972) 2975.

[5] (a) M.G. Kanatzidis, *Chem. Mater., 2* (1990) 353; (a) M.G. Kanatzidis and Y. Park, *Chem. Mater., 2* (1990) 99; (b) W. Hönle and H.G. von Schnering, *Z. Kristallogr. 179–180* (1987) 443; (c) H.G. von Schnering and G. Menge, *Z. Anorg. Allg. Chem., 481* (1981) 33; (d) W. Hönle and H.G. von Schnering, *Z. Kristallogr., 153* (1980) 339.

[6] B. Aronsson, L. Lundström and S. Rundquist, *Borides, Silicides and Phosphides*, Methuen, London, 1965.

[7] (a) R. Glaum and R. Gruehm, *Z. Kristallogr., 178* (1987) 72; (b) U. Flörke, *Z. Anorg. Allg. Chem., 502* (1983) 218; (c) M.W. Richardson and B. Noläng, *J. Cryst. Growth, 42* (1977) 90.

[8] (a) D.J. Olego, J. Baumann, R. Schachter, C. Michel, M. Kuck, S. Gersten and L.G. Polgar, *Phys. Rev. B., 31* (1985) 2240; (b) W. Schmettow, *Ph.D. Dissertation*, Münster University, 1975.

[9] W. Jeitschko and P.C. Donohue, *Acta Crystallogr., Sect. B, 28* (1972) 1893.

[10] C.J. Warren, *Ph.D. Dissertation*, Princeton University, 1994.

[11] S.S. Pons, D.J. Santure, R.C. Taylor and R.W. Rudolph, *Electrochim. Acta, 26* (1981) 365.

[12] (a) M. Björgvinsson, H.P.A. Mercier, K.M. Mitchell, G.J. Schrobilgen and G. Strohe, *Inorg. Chem., 32* (1993) 6046; (b) M. Björgvinsson, J.F. Sawyer and G.J. Schrobilgen, *Inorg. Chem., 30* (1991) 4238; (c) M. Björgvinsson and G.J. Schrobilgen, *Inorg. Chem., 30* (1991) 2540; (d) M. Björgvinsson, J.F. Sawyer and G.J. Schrobilgen, *Inorg. Chem., 26* (1987) 741; (e) R.C. Burns, L.A. Devereux, P. Granger and G.J. Schrobilgen, *Inorg. Chem., 24* (1985) 2615.

[13] (a) M.G. Kanatzidis and S.P. Huang, *Coord. Chem. Rev., 130* (1994) 509; (b) M.A. Ansari and J.A. Ibers, *Coord. Chem. Rev., 100* (1990) 223; (c) M. Draganjac, S. Dhingra, S.P. Huang and M.G. Kanatzidis, *Inorg. Chem., 29* (1990) 590; (d) M.G. Kanatzidis, *Comments Inorg. Chem., 10* (1990) 161.

[14] (a) A.A. Kudryavstev, *The Chemistry and Technology of Selenium and Tellurium*, 2nd edn., transl. by E.M. Elkin, Collet's, London, 1974; (b) R.H. Bube, *Annu. Rev. Mater. Sci., 20* (1990) 19; (c) H. Maier and J. Hesse, *J. Cryst. Growth 4* (1980) 145; (d) See any issue of *The Bulletin of the Selenium–Tellurium Development Association*, Grimbergen, Belgium.

[15] L.C. Roof and J.W. Kolis, *Chem. Rev., 93* (1993) 1037.

[16] R.G. Teller, L.J. Krause and R.C. Haushalter, *Inorg. Chem., 22* (1983) 1809.

[17] (a) E. Zintl and A. Harder, *Z. Phys. Chem. A, 154* (1931) 47; (b) E. Zintl, J. Goubeau and W. Dullenkopf, *Z. Phys. Chem. A, 154* (1931), 1; (c) E. Zintl and W. Dullenkopf, *Z. Phys. Chem. B, 16* (1932) 183, 195; (d) E. Zintl and S. Neumayr, *Z. Phys. Chem. B, 20* (1933) 272; (e) E. Zintl and S. Neumayr, *Z. Elektrochem., 39* (1933) 86; (f) E. Zintl and G. Brauer, *Z. Phys. Chem. B, 20* (1933) 245; (g) E. Zintl and E. Husemann, *Z. Phys. Chem. B, 21* (1933) 138; (h) E. Zintl, A. Harder and B. Dauth, *Z. Elektrochem., 40* (1934) 588; (i) E. Zintl and G. Woltersdorf, *Z. Elektrochem., 41* (1935) 876; (j) E. Zintl and G. Brauer, *Z. Elektrochem., 41* (1935) 297; (k) E. Zintl and A. Harder, *Z. Phys. Chem. B, 34* (1936) 238.

[18] (a) K. Suzuki, *Jpn. Kokai Tokkyo Koho*, 1989, 8 pp.; (b) K. Suzuki, *Jpn. Kokai Tokkyo Koho*, 1989, 6 pp.; (c) K. Kimura, K. Osada, M. Takenaga and T. Kurumisawa, *Jpn. Kokai Tokkyo Koho*, 1988, 8 pp.; (d) M. Takenaga, K. Kimura, M. Takao and N. Akahira, *Jpn. Kokai Tokkyo Koho*, 1987, 9 pp.

[19] A.I. Karapetyan and Sh.O. Amiryan, *Izv. Akad. Nauk Arm. SSR, Nauki Zemle, 39*(2) (1986) 13.

[20] J. Avraamides, *Chem. Aust., 58*(11) (1991) 484.

[21] G. Tunell and C. Ksandra, *J. Wash. Acad. Sci., 25* (1935) 32.

[22] G. Tunell and K. Murata, *Am. Mineral.*, *35* (1950) 959.
[23] M. Peacock and R. Thompson, *Bull. Geol. Soc. Am.*, *56* (1945) 1189.
[24] J. Fenner and D. Mootz, *J. Solid State Chem.*, *24* (1978) 367.
[25] H. Haendler, D. Mootz, A. Rabenau and G. Rosenstein, *J. Solid State Chem.*, *10* (1974) 175.
[26] M.A. Ansari, J.C. Bollinger and J.A. Ibers, *J. Am. Chem. Soc.*, *115* (1993) 3838.
[27] (a) M.A. Ansari, J.C. Bollinger and J.A. Ibers, *J. Am. Chem. Soc.*, *115* (1993) 3838; (b) S.S. Dhingra and R.C. Haushalter, *Inorg. Chem.*, *33* (1994) 2735.
[28] C.J. Warren, D.M. Ho, A.B. Bocarsly and R.C. Haushalter, *J. Am. Chem. Soc.*, *115* (1993) 6416.
[29] (a) $[Mg(N\text{-MeIm})_6]Sb_2S_{15}$: P.P. Paul, T.B. Rauchfuss and S.R. Wilson, *J. Am. Chem. Soc.*, *115* (1993) 3316; (b) $(C_3H_7)_4NSb_3S_5$ and $C_4H_8N_2Sb_4S_7$: J.B. Parise and Y. Ko, *Chem. Mater.*, *4*(6) (1992) 1446; (c) $CaSb_2S_4$, $Ca_2Sb_2S_5$ and $CaSb_4S_7$: T.N. Guliev, P.G. Rustamov and M.I. Chiragov, *Izv. Vyssh. Uchebn. Zaved., Khim. Khim. Tekhnol.*, *31*(6) (1988) 20; (d) $SrSb_4S_7 \cdot 6H_2O$: G. Cordier, H. Schäfer and C. Schwidetzky, *Z. Naturforsch.*, *39b* (1984) 131; (e) $RbSb_3S_5 \cdot H_2O$: K. Volk and H. Schäfer, *Z. Naturforsch.*, *34b* (1979) 172; (f) $Rb_2Sb_4S_7 \cdot H_2O$: G. Dittmar and H. Schäfer, *Z. Anorg. Allg. Chem.*, *441* (1978) 93; (g) $KSbS_2$: H.A. Graf and H. Schäfer, *Z. Anorg. Allg. Chem.*, *414* (1975) 211; (h) $K_2Sb_4S_7$: H.A. Graf and H. Schäfer, *Z. Naturforsch.*, *27b* (1972) 735.
[30] (a) $RbSb_3Se_5$: W.S. Scheldrick and H.J. Haeusler, *Z. Anorg. Allg. Chem.*, *557* (1988) 98; (b) $CsSbSe_2$: S. Kanishcheva, Yu.N. Mikhailov, V.B. Lazarev and N.A. Moshchalkova, *Dokl. Akad. Nauk SSSR*, *252*(4), (1980) 872; (c) $BaSb_2Se_4$: G. Cordier and H. Schäfer, *Z. Naturforsch.*, *34b*(8) (1979) 1053; (d) $KSbSe_2$; G. Dittmar and H. Schäfer, *Z. Naturforsch.*, *32b*(11) (1977) 1346.
[31] (a) M. Hansen and K. Anderko, *Constitution of Binary Alloys*, McGraw-Hill, New York, 1958; (b) R.P. Elliott, *Constitution of Binary Alloys, First Supplement*, McGraw-Hill, New York, 1965.
[32] K. Volk, G. Cordier, R. Cook and H. Schäfer, *Z. Naturforsch.*, *35b* (1980) 136.
[33] (a) M. Evain, F. Boucher, R. Brec, J. Rouxel, J.S. Jung and C.J. O'Connor, *Eur. J. Solid State Inorg. Chem.*, *29*(6) (1992) 1055; (b) J.S. Jung, B. Wu, E.D. Stevens and C.J. O'Connor, *J. Solid-State Chem.*, *94* (1991) 362.
[34] S. Geller, J.H. Wernick, *Acta Crystallogr.*, *12* (1959) 46.
[35] A.S. Skoropanov, V.F. Skums, S.A. Al'fer, E.A. Gusev and A.A. Vecher, *Z. Phys. Chem. (Leipzig)*, *268*(3) (1987) 545.
[36] C.J. Warren, S.S. Dhingra, D.M. Ho, R.C. Haushalter and A.B. Bocarsly, *Inorg. Chem.*, *33* (1994) 2709.
[37] T. Park and M.G. Kanatzidis, *Chem. Mater.*, *3*(5) (1991) 781.
[38] C.J. Warren, D.M. Ho, R.C. Haushalter and A.B. Bocarsly, *Angew. Chem. Int. Ed. Engl.*, *32* (1993) 1646.
[39] S.C. Critchlow and J.D. Corbett, *Inorg. Chem.*, *23* (1984) 770.
[40] V.O. Mundt, G. Becker, H.J. Wessely, H.J. Breunig and H. Kischkel, *Z. Anorg. Allg. Chem.*, *486* (1982) 70.
[41] D.B. Sharma and J. Donohue, *Acta. Crystallogr.*, *16* (1963) 891; A.G. Turner and F.S. Mortimer, *Inorg. Chem.*, *5* (1966) 906.
[42] H. Bärnighausen, T. von Volkmann and J. Jander, *Acta. Crystallogr.*, *21* (1966) 571.
[43] (a) T. Ito, N. Morimoto and S. Sadanaga, *Acta. Crystallogr.*, *5* (1952) 775; (b) E.J. Porter and G.M. Sheldrick, *J. Chem. Soc., Dalton Trans.*, (1972) 1347.
[44] A.M. Griffin, P.C. Minshall and G.M.J. Sheldrick, *J. Chem. Soc., Chem. Commun.*, (1976) 809.
[45] R. Faggiani, R.J. Gillespie and J.E. Vekris, *J. Chem. Soc., Chem. Commun.*, (1988) 902.
[46] T.J. Bastow and H.J. Whitfield, *J. Chem. Soc., Dalton Trans.*, (1973) 1739.
[47] R.K. McMullan, D.J. Prince and J.D. Corbett, *Inorg. Chem.*, *10*(8) (1971) 1749.
[48] (a) G. Mills, L. Zongguan and D. Meisl, *J. Phys. Chem.*, *92* (1988) 822; (b) G.G. Higashi and M.A. Kastner, *Phys. Rev. B*, *24* (1981) 2295; (c) R.A. Street, *Solid State Commun.* *34* (1980) 157; (d) R.J. Kobliska and S.A. Solin, *Phys. Rev. B.*, *8* (1973) 756; (e) B.T. Kolomiets, T.F. Mazets and Sh.M. Efendiev, *J. Non-Cryst. Solids*, *4* (1970) 45; (f) V.S. Ban and B.E. Knox, *J. Chem. Phys.*, *52* (1970) 248.
[49] (a) B.H. Christian, R.J. Gillespie and J.F. Sawyer, *Inorg. Chem.*, *20* (1981) 3410; (b) E.J. Porter and G.M. Sheldrick, *J. Chem. Soc., Dalton Trans.*, (1972) 1347; (c) W.J. Stec, W.E. Morgan, R.G. Alberidge and J.R. van Wazer, *Inorg. Chem.*, *11* (1972) 219; (d) W. von Lauer, M. Becke-Goehring and K. Sommer, *Z. Anorg. Allg. Chem.*, *371* (1969) 193; (e) T. Ito, N. Morimoto and R. Sadanaga, *Acta Crystallogr.*, *5* (1952) 775; (f) C.S. Lu and J. Donohue, *J. Am. Chem. Soc. 66* (1944) 818.
[50] (a) A.E. Nadzhip and L.D. Dudkin, *Inorg. Mater.*, *25* (1989) 1234; (b) M.R. Thuler, R.L. Benbow and Z. Hurych, *Chem. Phys.*, *71* (1982) 265; (c) B.M. Gol'tsman, V.A. Kudinov and I.A. Smirnov, *Semiconducting Thermoelectric Materials Based on Bi_2Te_3*, Nauka, Moscow, 1972; (d) M.M. Stasova and O.G. Karpinski, *J. Struct. Chem.*, *8* (1967) 69; (e) N.Kh. Abrikosov, V.F. Bankina and L.V. Poretskaya, *Semiconducting Compounds, Their Preparation and Properties*, Nauka, Moscow, 1967, p. 122; (f) S. Zalar, *Adv. Energy Convers.*, *2* (1962) 105; (g) A. Brown and B. Lewis, *J. Phys. Chem. Solids*, *23* (1962) 1597.
[51] W.S. Sheldrick and J. Kaub, *Z. Naturforsch.*, *40b* (1) (1985) 19.
[52] (a) W.S. Sheldrick and H.J. Häusler, *Z. Anorg. Allg. Chem.*, *561* (1988) 139; (b) W.S. Sheldrick and H.J. Häusler, *Z. Anorg. Allg. Chem.*, *538* (1986) 45; (c) W.S. Sheldrick and J. Kaub, *Z. Anorg. Allg. Chem.*, *535* (1986) 179; (d) W.S. Sheldrick and J. Kaub, *Z. Naturforsch.*, *40b*(9) (1985) 1130; (e) W.S. Sheldrick and J. Kaub, *Z. Naturforsch.*, *40b*(8) (1985) 1020; (f) W.S. Sheldrick and J. Kaub, *Z. Naturforsch.*, *40b*(5) (1985) 571.
[53] (a) M.A. Ansari, J.A. Ibers, S.C. O'Neal, W.T. Pennington and J.W. Kolis, *Polyhedron*, *11* (1992) 1877; (b) S.C. O'Neal, W.T. Pennington and J.W. Kolis, *Inorg. Chem.*, *31* (1992) 888; (c) S.C. O'Neal, W.T. Pennington and J.W. Kolis, *J. Am. Chem. Soc.*, *113* (1991) 710.
[54] R.C. Haushalter, *J. Chem. Soc., Chem. Commun.*, (1987) 196.
[55] C. Belin and H. Mercier, *J. Chem. Soc., Chem. Commun.*, (1987) 190.
[56] C. Belin, *C.R. Acad. Sci., Ser. C.*, *298* (1984) 691.
[57] B. Eisenmann and R. Zagler, *Z. Naturforsch.*, *42b* (1987) 1079.
[58] B. Krebs, S. Pohl and W. Schiwy, *Angew. Chem. Int. Edn. Engl.*, *9* (1970) 897.
[59] (a) S. Pohl and B. Krebs, *Z. Anorg. Allg. Chem.*, *424* (1976) 265; (b) B. Krebs and S. Pohl, *Z. Naturforsch.*, *26b* (1971) 853.
[60] B. Krebs and H.J. Jacobsen, *Z. Anorg. Allg. Chem.*, *421* (1976) 97.
[61] B. Krebs and H. Müller, *Z. Anorg. Allg. Chem.*, *496* (1983) 47.
[62] W. Schiwy, S. Pohl and B. Krebs, *Z. Anorg. Allg. Chem.*, *402* (1973) 77.
[63] B. Krebs, S. Pohl and W. Schiwy, *Z. Anorg. Allg. Chem. 393* (1972) 241.
[64] (a) W.S. Sheldrick and H.G. Braunbeck, *Z. Naturforsch.*, *44b* (1989) 851; (b) B. Krebs and H. Uhlen, *Z. Anorg. Allg. Chem.*, *549* (1987) 35.
[65] B. Eisenmann and H. Schäfer, *Z. Anorg. Allg. Chem.*, *491* (1982) 67.
[66] B. Eisenmann, H. Schwerer and H. Schäfer, *Mater. Res. Bull.*, *18* (1983) 1189.

[67] B. Eisenmann, H. Schrod and H. Schäfer, *Mater. Res. Bull., 19* (1984) 293.
[68] (a) S.S. Dhingra and R.C. Haushalter, *Polyhedron, 13* (1994) 2775; (b) B. Eisenmann, H. Schäfer and H. Schwerer, *Z. Naturforsch., 38b* (1983) 924.
[69] R. Teller, L. Krause and R.C. Haushalter, *Inorg. Chem., 22* (1983) 1809.
[70] B. Eisenmann, H. Schwerer and H. Schäfer, *Mater. Res. Bull., 18* (1983) 383.
[71] (a) M.A. Ansari, J.C. Bollinger and J.A. Ibers, *Inorg. Chem., 32* (1993) 231; (b) J.C. Huffman, J.P. Haushalter, A.M. Umarji, G.K. Shenoy and R.C. Haushalter, *Inorg. Chem., 23* (1984) 2312.
[72] B. Krebs and W. Schiwy, *Z. Anorg. Allg. Chem., 398* (1973) 63.
[73] A.F. Wells, *Structural Inorganic Chemistry*, Oxford University Press, Oxford, 5th edn., 1984.
[74] J. Peters and B. Krebs, *Acta Crystallogr., Sect. B, 38* (1982) 1270.
[75] J.W. Boon and C.H. MacGillavry, *Recl. Trav. Chim. Pays-Bas, 61* (1942) 910.
[76] J.A.A. Ketelaar, W.H. t'Hart, M. Moerel and D. Polder, *Z. Kristallogr., 101* (1939) 396.
[77] J. Weis, H. Schäfer and G. Schön, *Z. Naturforsch., 31b* (1976) 1336.
[78] K.J. Range, G. Mahlberg and S. Obenland, *Z. Naturforsch., 32b* (1977) 1354.
[79] P. Villars and L.D. Calvert, in L. Kacprzak (ed.), *Pearson's Handbook of Crystallographic Data For Intermetallic Phases*, Vol. 1, American Society for Metals, Materials Park, OH, 2nd edn., 1991, pp. 292–293.
[80] S.S. Dhingra and R.C. Haushalter, *Chem. Mater., 6* (1994) 2376.
[81] A. Meerscaut and J. Rouxel, in J. Rouxel (ed.), *Crystal Chemistry and Properties of Materials with Quasi One-Dimensional Structures*, Reidel, Dordrecht, 1986, pp. 205–279.
[82] (a) S. Harris and R.R. Chianelli, *J. Catal., 86* (1984) 400; (b) R.R. Chianelli, T.A. Pecoraro, T.R. Halbert, W.H. Pan and E.I. Stiefel, *J. Catal., 86* (1984) 226; (c) T.A. Pecoraro and R.R. Chianelli, *J. Catal., 67* (1981) 430.
[83] (a) H. Eckert, *Angew. Chem. Int. Edn. Engl., 28* (1989) 1723; (b) N. Yamada, N. Ohno, N. Akahira, K. Nishiuchi, K. Nagata and M. Takao, *Proc. Int. Symp. on Optical Memory, 1987*, in *Jpn. J. Appl. Phys., 26 (Suppl. 4)* (1987) 61: (c) R. Zallen, *Physics of Amorphous Solids*, Wiley, New York, 1983; (d) D. Strand and D. Adler, *Proc. Soc. Photo-Instrum. Eng., 420* (1983) 200.
[84] M.G. Kanatzidis, *Chem. Mater., 2* (1990) 353.
[85] R.H. Moss, *J. Cryst. Growth, 68* (1984) 78.
[86] A.H. Cowley, B.L. Benac, J.G. Ekerdt, R.A. Jones, K.B. Kidd, J.Y. Lee and J.E. Miller, *J. Am. Chem. Soc., 110* (1988) 6248.
[87] A.H. Cowley and R.A. Jones, *Angew. Chem. Int. Edn. Engl., 28* (1989) 1208.
[88] G.E. Coates, *J. Chem. Soc.*, (1951) 2003.
[89] M.A. Banks, O.T. Beachley, Jr., H.J. Gysling and H.R. Luss, *Organometallics, 9* (1990) 1979.
[90] M.B. Power, J.W. Ziller, A.N. Tyler and A.R. Barron, *Organometallics, 11* (1992) 1055.
[91] B. Eisenmann and A. Hofmann, *Z. Kristallogr., 197* (1991) 145.
[92] (a) M. Leon, J.M. Merino and J.L. Martin de Vidales, *J. Mater. Sci., 27*(16) (1992) 4495; (b) G.D. Guseinov, G.I. Iskanderov, Z.A. Aliev, T.K. Kasumov and T.Sh. Dzhafarova, *Neorg. Mater., 27*(9) (1991) 1972; (c) G. Bocelli, G. Calestani, O. DeMelo, F. Leccabue, C. Pelosi and B.E. Watts, *J. Cryst. Growth, 113*(3–4) (1991) 663; (d) I.V. Bodnar, *Neorg. Mater., 27*(10) (1991) 2068; (e) M. Guittard, J. Rivet, F. Alapini, A. Chilouet and A.M. Loireau-Lozac'h, *J. Less-Common Met., 170*(2) (1991) 373; (f) A.T. Nagat, G.A. Gamal and S.A. Hussein, *Cryst. Res. Technol., 26*(1) (1991) 19; (g) A.T. Nagat, G.A. Gamal and S.A. Hussein, *Phys. Status Solidi A, 120*(2) (1990) K163; (h) I.V. Bodnar and N.S. Orlova, *Cryst. Res. Technol., 21*(8) (1986) 1091.
[93] (a) $CdGa_2Te_4$: P.M. Nikolic and S.M. Stojilkovic, *J. Phys. C., 14*(19) (1981) L551; (b) $HgGa_2Te_4$: E. Agostinelli, L. Gastaldi and S. Viticoli, *Mater. Chem. Phys., 12*(4) (1985) 303.
[94] B. Panzer, K.J. Range and M. Zabel, *J. Less-Common Met., 106*(2) (1985) 305.
[95] C.J. Warren, D.M. Ho, R.C. Haushalter and A.B. Bocarsly, *J. Chem. Soc., Chem. Commun.*, (1994) 361.
[96] L. Pauling, *The Nature of the Chemical Bond*, Cornell University Press, Ithaca, NY, 3rd edn., 1960.
[97] (a) M. Julien-Pouzol, S. Jaulmes, M. Guittard and F. Alapini, *Acta Crystallogr., Sect. B, 35* (1979) 2848; (b) F. Alapini, J. Flahaut, M. Guittard, S. Jaulmes and M. Julien-Pouzol, *J. Solid-State Chem., 28* (1979) 309.
[98] S.A. Semiletov and V.A. Vlasov, *Kristallografiya, 8* (1963) 877.
[99] V.H. Hahn and W. Klingler, *Z. Anorg. Allg. Chem., 259* (1949) 135.
[100] K. Cisar and J.D. Corbett, *Inorg. Chem., 16* (1977) 632.
[101] J.C. Huffman and R.C. Haushalter, *Z. Anorg. Allg. Chem., 518* (1984) 203.
[102] W.C. Hamilton and J.A. Ibers, *Hydrogen Bonding in Solids*, W.A. Benjamin, New York, 1968, pp. 14–18.
[103] H. Deiseroth, *Z. Naturforsch., 35b* (1980) 953.
[104] B. Krebs, *Angew. Chem., Int. Edn. Engl. 22* (1983) 113.
[105] E.R. Franke and H. Schäfer, *Z. Naturforsch., 37b* (1972) 1308.
[106] V.W. Klee and H. Schäfer, *Z. Anorg. Allg. Chem., 479* (1981) 125.
[107] B. Eisenmann, A. Hofmann and R. Zagler, *Z. Naturforsch., 45b* (1990) 125.
[108] H.J. Deiseroth, D. Müller and H. Hahn, *Z. Anorg. Allg. Chem., 525* (1985) 163.
[109] W. Hönle, G. Kühn and H. Neumann, *Z. Anorg. Allg. Chem., 532* (1986) 150.
[110] V.G. Roos, G. Eulenberger and H. Hahn, *Z. Anorg. Allg. Chem., 396* (1973) 284.
[111] J.H. Zhang, A.J. van Duyneveldt, J.A. Mydosh and C.J. O'Connor, *Chem. Mater., 1* (1989) 404.
[112] C.J. Warren, S.S. Dhingra, R.C. Haushalter and A.B. Bocarsly, *J. Solid-State Chem., 112* (1994) 340.
[113] C.J. Warren, R.C. Haushalter and A.B. Bocarsly, *Chem. Mater., 6* (1994) 780.
[114] N.N. Greenwood and A. Earnshaw, *Chemistry of the Elements*, Pergamon, Oxford, 1990, p. 643.
[115] (a) W. Schmettow and H.G. von Schnering, *Angew. Chem. Int. Edn. Engl., 16* (1977) 857; (b) H.G. Schnering, in A. Cowley (ed.), *Rings, Clusters and Polymers of the Main Group Elements*, in ACS Symp. Ser., *232* (1983) 69.
[116] C.H.E. Belin, *J. Am. Chem. Soc., 102* (1980) 6036.
[117] (a) R.C. Haushalter, *J. Chem. Soc., Chem. Commun.*, (1987) 196; (b) B. Eisenmann and R. Zagler, *Z. Naturforsch., 42b* (1987) 1079; (c) C. Belin, *C.R. Acad. Sci., Ser. C., 298* (1984) 691.
[118] P. Böttcher, *Angew. Chem. Int. Edn. Engl., 27* (1988) 759.
[119] (a) F. Alapini, J. Flahaut, M. Guittard, S. Jaulmes and M. Julien-Pouzol, *J. Solid-State Chem., 28* (1979) 309; (b) M. Julien-Pouzol, S. Jaulmes and F. Alapini, *Acta Crystallogr., Sect. B, 33* (1977) 2270.
[120] (a) B. Eisenmann, H. Schwerer and H. Schäfer, *Mater. Res. Bull., 18* (1983) 383; (b) C. Brinkmann, B. Eisenmann and H. Schäfer, *Mater. Res. Bull., 20* (1985) 299.
[121] S.S. Dhingra and R.C. Haushalter, unpublished results.

[122] R.C. Burns and J.D. Corbett, *Inorg. Chem.*, *20* (1981) 4433.
[123] R.C. Haushalter, *Angew. Chem. Int. Edn. Engl.*, *24* (1985) 433.
[124] S.S. Dhingra, C.J. Warren, R.C. Haushalter and A.B. Bocarsly, *Chem. Mater.*, *6* (1994) 2382.
[125] (a) K.W. Kim and M.G. Kanatzidis, *Inorg. Chem.*, *30* (1991) 1969; (b) M.G. Kanatzidis and Y. Park, *Chem. Mater.*, *2* (1990) 99; (c) G. Krauter, F. Weller and K. Dehnicke, *Z. Naturforsch.*, *44b* (1989) 444, and references cited therein.
[126] (a) J.M. McConnachie, M.A. Ansari, J.C. Bollinger, R.J. Salm and J.A. Ibers, *Inorg. Chem.*, *32* (1993) 3201; (b) U. Müller, C. Grebe, B. Neumüller, B. Schreiner and K. Dehnicke, *Z. Anorg. Allg. Chem.*, *619* (1993) 500.
[127] R. Fenn, J. Oldham and D. Phillips, *Nature*, *198* (1963) 381.
[128] K. Aurivillins and C. Stalhandske, *Acta. Crystallogr., Sect B*, *30* (1974) 1907.
[129] (a) S.L. Suib, *Chem. Rev.*, *93* (1993) 803; (b) G.D. Stucky and J.E. MacDougall, *Science 247* (1990) 669; (c) P.A. Jacobs and R.A. van Santen (eds.), *Zeolites: Facts, Figures, Future*, Parts A and B Elsevier, Amsterdam, 1989; (d) G.A. Ozin, A. Kuperman and A. Stein, *Angew. Chem. Int. Edn. Engl.*, *28* (1989) 359; (e) J.M. Thomas, *Angew. Chem. Int. Edn. Engl.*, *27* (1988) 1673; (f) J.M. Newsam, *Science*, *231* (1986) 1093; (g) S.T. Wilson, B.M. Lok, C.A. Messina, T.R. Cannan and E.M. Flanigen, *J. Am. Chem. Soc.*, *104* (1982) 1146.
[130] R.L. Bedard, S.T. Wilson, L.D. Vail, J.M. Bennett and E.M. Flanigen, in *Zeolites: Facts, Figures, Future*, Part A, P.A. Jacobs and R.A. van Santen, (eds.), Elsevier, Amsterdam, 1989, p. 375.
[131] S. Dhingra and M.G. Kanatzidis, *Science*, *258* (1992) 1769.
[132] J.B. Parise, *Science*, *251* (1991) 293.
[133] C.J. Warren, R.C. Haushalter and A.B. Bocarsly, *J. Alloys Compd.* in press.
[134] W.S. Sheldrick and B. Schaaf, *Z. Naturforsch.*, *49b* (1994) 993.
[135] P. Cherin and P. Unger, *Acta Crystallogr.*, *23* (1967) 670.
[136] R.C. Haushalter and L.A. Mundi, *Chem. Mater.*, *4* (1992) 31.